



ČESKÉ VYSOKÉ UČENÍ TECHNICKÉ V PRAZE

FAKULTA ELEKTROTECHNICKÁ

Czech Technical University in Prague

Faculty of Electrical Engineering

Department of Electric Drives and Traction

Diploma Thesis

Implementation of Field Oriented Control in Simulink

Implementace vektorového řízení pomocí Simulinku

Alberto Alvarez

© 2020 CTU Prague



# MASTER'S THESIS ASSIGNMENT

## I. Personal and study details

Student's name:	<b>Alvarez Alberto</b>	Personal ID number:	<b>472740</b>
Faculty / Institute:	<b>Faculty of Electrical Engineering</b>		
Department / Institute:	<b>Department of Electric Drives and Traction</b>		
Study program:	<b>Electrical Engineering, Power Engineering and Management</b>		
Specialisation:	<b>Electrical Drives</b>		

## II. Master's thesis details

Master's thesis title in English:  
**Implementation of Field Oriented Control in Simulink**

Master's thesis title in Czech:  
**Implementace vektorového řízení pomocí Simulinku**

Guidelines:

- 1) Make a survey about models of induction motor used for its simulation
- 2) Make a survey about field oriented control strategies
- 3) Create simulation model of FOC for induction motor in Simulink
- 4) Evaluate validity of the simulation by simulation of drive transients

Bibliography / sources:

- [1] MOHAN, Ned. Power electronics: a first course. Hoboken: Wiley, 2012.
- [2] MOHAN, Ned. Advanced electric drives: analysis, control, and modeling using MATLAB / Simulink. Hoboken: Wiley, 2014
- [3] MatLab documentation - [www.mathworks.com](http://www.mathworks.com)

Name and workplace of master's thesis supervisor:  
**Ing. Jan Bauer, Ph.D., Department of Electric Drives and Traction, FEE**

Name and workplace of second master's thesis supervisor or consultant:  
\_\_\_\_\_

Date of master's thesis assignment: **20.09.2019**      Deadline for master's thesis submission: **14.08.2020**

Assignment valid until: **30.09.2021**

\_\_\_\_\_  
Ing. Jan Bauer, Ph.D.  
Supervisor's signature

\_\_\_\_\_  
Head of department's signature

\_\_\_\_\_  
prof. Mgr. Petr Páta, Ph.D.  
Dean's signature

## III. Assignment receipt

The student acknowledges that the master's thesis is an individual work. The student must produce his thesis without the assistance of others, with the exception of provided consultations. Within the master's thesis, the author must state the names of consultants and include a list of references.

\_\_\_\_\_  
Date of assignment receipt

\_\_\_\_\_  
Student's signature

## Declaration

I hereby declare that this thesis “Implementation of Field Oriented Control in Simulink” is the result of my own work and all the sources I used in the list of references, in accordance with the Methodological Instructions of Ethical Principle in the preparation of University thesis.

In Prague: \_\_\_\_\_

\_\_\_\_\_

Signature

## **Abstract**

Induction machines are one of the most widely used electric machines on many industrial and transportation applications. It is, therefore, important to have a facility to control these machines for the wide range of applications. On the other hand, it is possible to control DC machines with much simpler control schemes, but their technical drawbacks do not make them the preferable choice for the industry nowadays. Many control strategies have been developed for the speed and torque control of induction machines and more research is still ongoing using more modern techniques, such as “fuzzy logic” and “neural networks”. One of the most widely used control techniques is the “field-oriented control”, which is the topic of this thesis. With the parameters of a real induction machine, we implemented a control scheme based on the field-oriented control in the Simulink software. Various scenarios were applied to the controller in order to study its functioning and possible improvements. Furthermore, a speed estimation part was implemented for a sensorless control of the machine.

Keywords: induction machine, electric drives, Simulink, field-oriented control, vector control, sensorless control.

## **Abstrakt**

Indukční stroje jsou jedním z nejpoužívanějších elektrických strojů v mnoha průmyslových a dopravních aplikacích. Je proto důležité mít zařízení pro jejich ovládání. Naproti tomu, DC stroje je možné řídit pomocí mnohem jednodušších schémat, ale kvůli jejich technickým nevýhodám se v současnosti nejeví jako nejlepší volba pro průmyslové použití. Pro řízení rychlosti a točivého momentu indukčních strojů bylo vyvinuto mnoho řídicích strategií a stále probíhá další výzkum pomocí modernějších technik, jako například „Fuzzy logic“ nebo neuronové sítě. Tématem práce je plem orientované vektorové řízení, které je jedním z nejpoužívanějších způsobů řízení. Implementovali jsme schéma s plem orientovaným řízením v softwaru Simulink na indukční stroj se skutečnými parametry. Pro zkoumaný řadič jsme vyzkoušeli různé scénáře s cílem zjistit jeho fungování a možná vylepšení. Rovněž jsme implementovali bezsenzorové řízení stroje s odhadem otáček.

Klíčová slova: indukční stroj, elektrické pohony, Simulink, plem orientované řízení, vektorové řízení, bezsenzorové řízení.

# Table of Contents

Introduction.....	1
Chapter 1 The Induction machine.....	2
1.0.1 Induction machine characteristics.....	2
1.1 Induction machine: mathematical model.....	3
1.1.1 Space Vector.....	3
1.1.2 Space Quantities.....	6
1.1.2.1 Voltage Equations.....	6
1.1.2.2 Flux Equations.....	7
1.1.2.3 Electrical power and torque equations.....	8
1.1.2.4 Acceleration equation.....	9
Chapter 2 Field Oriented Control Strategies.....	10
2.1 Field Oriented Control.....	11
2.2 Direct Torque Control.....	13
2.2.1 Torque Expressions with Stator and Rotor Fluxes.....	13
2.2.2 Control Scheme.....	14
2.2.3 Control Strategy.....	15
2.3 Feedback Linearization.....	17
2.4 Passivity Based Control.....	17
Chapter 3 Simulink Model.....	18
3.1 Equations for modeling IM.....	19
3.2 Simulink model of the IM.....	21
3.4 Field Oriented Control.....	24
3.4.1 Flux Estimation.....	25
3.4.2 Speed Estimator.....	25
3.5 Full control scheme.....	27
3.6 Simulations.....	30
3.6.1 Case 1: Constant speed, speed step and load step.....	30
3.6.2 Case 2: Speed Ramp, constant speed, negative speed step and load torque step.....	33
3.6.3 Case 3: Speed Estimator at lower speeds.....	37
3.6.4 Case 4: Speed step and load step. W/O Estimator.....	38
Conclusions.....	41
Bibliography.....	42

## List of figures

Figure 1-1 Three phases and space vector. [5] .....	4
Figure 1-2 d-q axis and space vector. [5] .....	5
Figure 2-1 Induction Machine control classifications. [5] .....	10
Figure 2-2 Scheme for the implementation of field-oriented control. [2] .....	12
Figure 2-3 Direct Torque Control basic scheme. [2] .....	15
Figure 2-4 Flux-linkage circle division into sectors $\kappa$ determined by the voltage vectors. [2].....	16
Figure 2-5 Optimal Switching Table. [2].....	17
Figure 3-1 $\alpha$ and $\beta$ components of supply voltage. ....	21
Figure 3-2 Modelling for $i_{s\alpha}$ and $\psi_{R\alpha}$ .....	22
Figure 3-3 Modelling for $i_{s\beta}$ and $\psi_{R\beta}$ .....	23
Figure 3-4 Modelling of torque and speed section.....	23
Figure 3-5 Complete IM model. ....	24
Figure 3-6 $\alpha$ - $\beta$ to d-q transformation.....	24
Figure 3-7 Rotor Flux estimation blocks. ....	25
Figure 3-8 Speed Estimator general scheme. ....	26
Figure 3-9 Speed Estimator Simulink model.....	27
Figure 3-10 Implemented general control scheme. ....	28
Figure 3-11 Full Simulink schematic.....	29
Figure 3-12 Reference and actual flux for case 1.....	30
Figure 3-13 Flux in polar coordinates for case 1.....	31
Figure 3-14 Reference and actual $i_q$ for case 1.....	31
Figure 3-15 Machine, reference and Estimated Speeds for case 1. ....	32
Figure 3-16 Load torque, Machine torque and Electromagnetic torque for case 1. ....	33
Figure 3-17 Reference and actual flux for case 2.....	34
Figure 3-18 Flux in polar coordinates for case 2.....	34
Figure 3-19 Reference and actual $i_q$ for case 2.....	35
Figure 3-20 Machine, reference and Estimated Speeds for case 2. ....	36
Figure 3-21 Load torque, Machine torque and Electromagnetic torque for case 2. ....	36
Figure 3-22 Machine, reference and Estimated Speeds for case 3. ....	37
Figure 3-23 Reference and actual flux for case 4.....	38
Figure 3-24 Measured Flux in polar coordinates for case 4.....	38
Figure 3-25 Reference and actual $i_q$ for case 4.....	39
Figure 3-26 Machine and reference Speeds for case 4.....	39
Figure 3-27 Load torque, Machine torque and Electromagnetic torque for case 4. ....	40

## Introduction.

The topic to work is the implementation of vector control of asynchronous motor on Simulink. The scope of this work goes from the description and mathematical model of the asynchronous motor or Induction machine to the implementation of a field-oriented control scheme of the motor based on real machine parameters.

For this purpose, we start with a brief description of the induction machine as, it will be explained further, is one of the most used electromechanical energy conversion devices. We dedicated the first section of this document to describe the basic working principle and the difference from the synchronous machine.

Secondly, a mathematical model of the machine was derived based on its physical principals. Also, this model should be adapted for the control scheme intended for implementation. For this use, a dynamic model should be defined as the static models and control schemes don't offer a wide range of controllability.

After describing machine principles, we continue describing most used IM machine control methods: Field Oriented Control and Direct Torque Control. Both methods are based on the dynamic behavior of the machine and so the control is possible in a wide range of situations. Also, some brief explanation of more modern control techniques is given.

Finally, the model of the induction machine is developed on the Simulink software and a control scheme is created. Various cases are designed to verify the behavior of the controller and the dynamic response of the machine. The controller also includes a speed estimator, so the model works as a sensor less control scheme. After it, every case is described and

## Chapter 1 The Induction machine.

For many years, the DC motors were the ideal machines for many industrial and transport applications even after the AC was established as the standard for electrical systems. This was mainly because of its wide speed control range and excellent operational characteristics. The essential disadvantage is the mechanical commutator on the machine rotor which limits the power and speed of the motor, increases the inertia and the axial length and requires periodic maintenance.

The induction machines are more simpler and rugged in construction compared to DC machines as they don't possess any commutator or slip rings. Albeit knowing this fact, the induction machine didn't substitute DC machines immediately. The current and speed relations not being linear as in DC which make their control characteristics very different. This didn't make possible to use AC machines for variable speed applications. However, with the development of power electronics it is possible to make these machines as versatile and economical as a DC drive.

### 1.0.1 Induction machine characteristics.

An induction machine carries alternating currents in both the stator and rotor windings with the stator connected to a balanced three-phase supply. The windings in the rotor side are usually internally short-circuited or connected through slip rings to a passive external circuit. The main characteristic of this machine is that rotor currents are induced by the stator by electromagnetic induction.

The stator of a three-phase induction machine is similar to that of a synchronous machine. When balanced three-phase currents of frequency  $f_s$  Hz are applied, the stator produces a magnetic field rotating at synchronous speed given by:

$$n_s = \frac{120f_s}{p_f} \quad (1.1)$$

Where  $n_s$  is in r/min and  $p_f$  is the number of pair poles.

Because of the lack of an excitation system as in synchronous machines, the induced voltage on the rotor doesn't have the same speed as the stator magnetic field. This relative speed between the stator and rotor is called slip and its necessary to generate positive torque in the machine. The current on the rotor is given by the induced voltage divided by the rotor impedance at the frequency of the same induced voltage  $f_r$ . The slip parameter can be calculated by the following expression:

$$s = \frac{n_s - n_r}{n_s} \quad (1.2)$$

This is a very important dynamic parameter of the machine as it increases or decreases according to the load. In a no-loaded machine, the slip can be neglected but it increases with an increasing load.



## 1.1 Induction machine: mathematical model.

In this section we will develop the mathematical model of the induction machine intended for simulation, as this is necessary for the development of any control system. This consists of the differential equations describing the electromagnetic relationships of the stator and the rotor as well as the equation of motion and electromechanical conversion. We should consider a dynamic model as its intended for better control performance. For this case, some assumptions should be made:

- The machine is supply by a symmetrical AC source.
- The machine consist of 3 stator [S] windings and 3 rotor [R] windings.
- Existence of mutual inductances  $M$  between windings and ohmic resistance in all windings.
- The rotor has a symmetrical structure. A fixed frame  $(\alpha, \beta, 0)$  or rotational reference frame  $(d, q, 0)$  could be applied.
- The rotor speed is not fixed but varies with load.
- The IM does not have an excitation winding, so the dynamics of the rotor are given by the slip. [9]

Also, according to the control method that would be applied, various reference frames could be considered depending on the variables to control or also state quantities. For our case, the reference frame is called “field reference frame” or “rotor-flux reference frame.”

### 1.1.1 Space Vector

The space vector theory is the simplest method for describing the electric machine dynamics or any three-phase system. It is the core for all vector control techniques. In this section, we will describe shortly the application of this method.

Consider a current  $i$  flowing through a coil, current vector  $\mathbf{i}$  is collinear with the magnetic axis of its coil. The direction of the current vector is defined by the actual position of the coil and the magnitude is the instantaneous value current (AC or DC). [3]

Now, if we consider a three phase AC machine with three symmetrical currents  $i_a, i_b, i_c$  flowing through its coils. The axes of the three phases are mutually displaced in space of  $120^\circ$ . If we do a vector addition, from these currents we obtain a single space vector of the phase currents:

$$\mathbf{i} = \mathbf{i}_a + \mathbf{i}_b + \mathbf{i}_c \quad (1.3)$$

The space vector is confined to a plane, with the  $i_a$  current vector along or colinear the real axis as shown in figure 1.

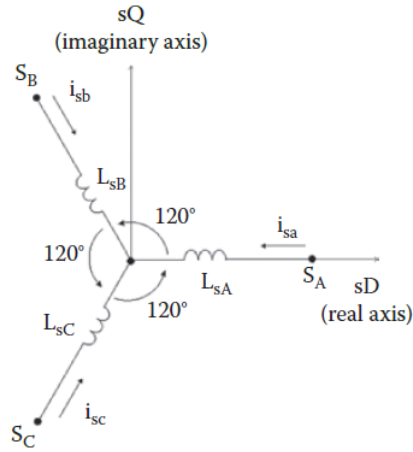


Figure 1-1 Three phases and space vector. [5]

Representing vectors  $i_b$  and  $i_c$  on the complex plane we can write with Euler notation:

$$i_b = i_b e^{j120^\circ} = \mathbf{a} i_b \quad (1.4)$$

$$i_c = i_c e^{j240^\circ} = \mathbf{a}^2 i_c \quad (1.5)$$

Rewriting expression 3 we obtain:

$$i = i_a + \mathbf{a} i_b + \mathbf{a}^2 i_c \quad (1.6)$$

Finally, to represent the phase quantity of the space vector in a poly-phase machine:

$$i_s = \frac{2}{3} (i_a + \mathbf{a} i_b + \mathbf{a}^2 i_c) = |i_s| e^{j\alpha_s} = i_{sD}(t) + j i_{sQ}(t) \quad (1.7)$$

Where:

$|i_s|$  is the amplitude of the space vector.

$\alpha_s$  is the angle of the current space vector from the sD axis.

$i_{sD}(t)$  and  $i_{sQ}(t)$  are, respectively, the instantaneous values of the sD and sQ components of the current space-vector corresponding to the real and imaginary components of the space-vector in the complex plane.

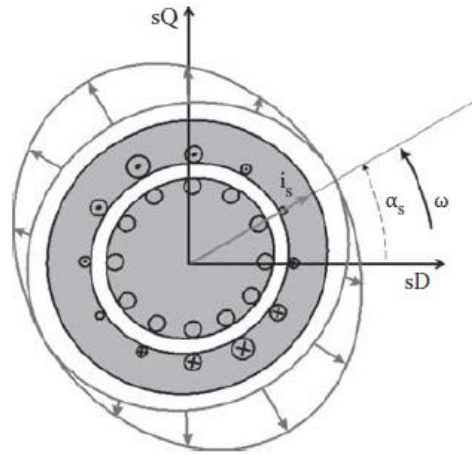


Figure 1-2 d-q axis and space vector. [5]

If we define a given space vector, we can also define a new orthogonal plane (d-q) and then obtain its direct (sD or real) and quadrature (sQ or imaginary) components, note that all phase quantities can be directly computed from the three-phase variables.

This transformation is also called the 3→2 transformation or Park transformation if a rotational reference frame and Clarke transformation if a fixed reference frame is chosen. One of the advantages offered by the space-vector quantity is the possibility to perform a coordinate transformation by means of a vector rotation. We can use stator reference frame, in the rotor reference frame, and in a general reference frame. By using this last general reference frame, the equations can be also written in the stator flux-linkage reference frame, the rotor flux-linkage reference frame, and the magnetizing flux-linkage reference frame. [5]

For control purposes, in AC machines under balanced sinusoidal steady-state conditions, we can replace the three windings by a single hypothetical equivalent winding that produced the same mmf distribution in the air gap. After it, we can decompose the single winding quantities into the two orthogonal axis (or windings) such that the torque and the flux within the machine can be controlled independently. In this way, we can develop a control strategy for the AC machine similar to the DC machine. [5]

### 1.1.2 Space Quantities.

Depending on chosen reference frame voltage, current and flux linkage equations can be defined. For our case, we will start by defining the space quantities in the stator reference frame. A more detailed explanation for this will be given in the next chapter.

#### 1.1.2.1 Voltage Equations.

The voltage equations for individual stator phase windings are given as:

$$u_{sa} = i_{sa}R_s + \frac{d\psi_{sa}}{dt}$$
$$u_{sb} = i_{sb}R_s + \frac{d\psi_{sb}}{dt}$$
$$u_{sc} = i_{sc}R_s + \frac{d\psi_{sa}}{dt}$$

Where  $u_s$  and  $i_s$  are the stator voltages in [V] and currents [A] for a given phase respectively,  $R_s$  is the stator resistance in [ $\Omega$ ] and  $\psi$  is the stator flux linkage.

In a general way, we can express stator voltage space vector as:

$$\mathbf{u}_s = \mathbf{i}_s R_s + \frac{d\boldsymbol{\psi}_s}{dt} \quad (1.8)$$

The voltage expression in  $\alpha$ - $\beta$  coordinates:

$$u_{s\alpha} = i_{s\alpha}R_s + \frac{d\psi_{s\alpha}}{dt} \quad (1.9)$$

$$u_{s\beta} = i_{s\beta}R_s + \frac{d\psi_{s\beta}}{dt} \quad (1.10)$$

The voltage expression in d-q coordinates:

$$u_{sd} = i_{sd}R_s + \frac{d\psi_{sd}}{dt} - \omega_d \psi_{sq} \quad (1.11)$$

$$u_{sq} = i_{sq}R_s + \frac{d\psi_{sq}}{dt} + \omega_d \psi_{sd} \quad (1.12)$$

The term  $\omega_d$  is the speed of the dq reference frame relative to the actual physical stator winding speed. If the reference frame is fixed in the stator, this term is 0.

The same way as in the stator, the rotor voltage space vector can be expressed as:

$$\mathbf{u}_r = \mathbf{i}_r R_r + \frac{d\boldsymbol{\psi}_r}{dt} + \omega_d \boldsymbol{\psi}_r \quad (1.13)$$

Note that rotor voltage is 0 if the machine have a squirrel cage rotor.

The rotor voltage expression in  $\alpha$ - $\beta$  coordinates:

$$u_{R\alpha} = i_{R\alpha} R_R + \frac{d\psi_{R\alpha}}{dt} \quad (1.14)$$

$$u_{R\beta} = i_{R\beta} R_R + \frac{d\psi_{R\beta}}{dt} \quad (1.15)$$

The voltage expression in d-q coordinates:

$$u_{Rd} = i_{Rd} R_s + \frac{d\psi_{Rd}}{dt} - \omega_d \psi_{Rq} \quad (1.16)$$

$$u_{Rq} = i_{Rq} R_R + \frac{d\psi_{Rq}}{dt} + \omega_d \psi_{Rd} \quad (1.17)$$

The term  $\omega_d$  is the speed of the dq reference frame relative to the actual physical stator winding speed. But if the reference frame is fixed in the rotor, this term is 0.

### 1.1.2.2 Flux Equations.

When obtaining the flux equations, we can verify the real advantage of using the space vector method and choosing the correct reference frame. We start considering that all six of the stator and rotor phase currents influence the asynchronous machine's total flux linkage. This relation can be represented with the following set of equations:

$$\psi_{Sa} = (L_{S\sigma} + L_p) i_{Sa} + L_{SM} i_{Sb} + M_S i_{Sc} + M_{SR} \cos(\theta_R) i_{Ra} + M_{SR} \cos\left(\theta_R + \frac{2\pi}{3}\right) i_{Rb} + M_{SR} \cos\left(\theta_R + \frac{4\pi}{3}\right) i_{Rc}$$

$$\psi_{Sb} = (L_{S\sigma} + L_p) i_{Sb} + L_{SM} i_{Sa} + M_S i_{Sc} + M_{SR} \cos\left(\theta_R + \frac{4\pi}{3}\right) i_{Ra} + M_{SR} \cos(\theta_R) i_{Rb} + M_{SR} \cos\left(\theta_R + \frac{2\pi}{3}\right) i_{Rc}$$

$$\psi_{Sc} = (L_{S\sigma} + L_p) i_{Sc} + L_{SM} i_{Sa} + M_S i_{Sb} + M_{SR} \cos\left(\theta_R + \frac{2\pi}{3}\right) i_{Ra} + M_{SR} \cos\left(\theta_R + \frac{4\pi}{3}\right) i_{Rb} + M_{SR} \cos(\theta_R) i_{Rc}$$

Equations 1.18, 1.19 and 1.20.

Where  $L_{S\sigma}$  is the leakage inductance of the stator,  $L_p$  is the main or self-inductance of the phase,  $L_{SM}$  is the mutual inductance between the stator windings,  $M_{SR}$  is the maximum value of the mutual inductance between the stator and rotor windings,  $\theta_R$  is the angle between the magnetic axes of the rotor and stator, and the instantaneous phase currents of the rotor are  $i_{Ra}$ ,  $i_{Rb}$ ,  $i_{Rc}$ . Due to symmetry reasons, the values of leakage inductance, self-inductance and mutual

inductance between the stator are constant whatever stator and rotor winding is considered. However, the mutual inductance between the stator and the rotor windings varies with the rotor angle. [2]

If we use the space vector for the stator flux linkage:

$$\boldsymbol{\psi} = \frac{2}{3}(\mathbf{a}^0\psi_a + \mathbf{a}\psi_b + \mathbf{a}^2\psi_c) \quad (1.21)$$

By using equations (1.18 through 1.20) and (4.11) and rearranging, the stator flux-linkage space vector can be expressed as a function of the stator current space-vector and the rotor current space-vector in the stator reference frame:

For the flux linkages, the equations used to describe the machine are:

$$\boldsymbol{\psi}_s = \mathbf{i}_s L_s + \mathbf{i}_r L_M \quad (1.22)$$

$$\boldsymbol{\psi}_r = \mathbf{i}_s L_M + \mathbf{i}_r L_R \quad (1.23)$$

Where  $L_s = L_{SM} + L_{S\sigma}$  is the total three-phase inductance of the stator winding per phase,  $L_{Sm}$  is the mutual inductance between the stator windings and  $L_{S\sigma}$  is the leakage inductance of the stator. For the rotor, by analogy,  $L_R = L_{RM} + L_{R\sigma}$ . In these equations we consider the respective rotor and stator space current vector.

We can verify that instead of the more complex Equations 1.18 through 1.20, a simple space vector representation can be applied as presented by Equations 1.22 and 1.23. The space-vector approach offers a simple and efficient method to achieve a control model solution for an asynchronous electric machine. [2]

### 1.1.2.3 Electrical power and torque equations

The instantaneous Power input to the stator is:

$$p_s = u_{sa}i_{sa} + u_{sb}i_{sb} + u_{sc}i_{sc} \quad (1.22)$$

For the rotor we have:

$$p_r = u_{ra}i_{ra} + u_{rb}i_{rb} + u_{rc}i_{rc} \quad (1.23)$$

The electromagnetic torque developed is obtained as the power as the power associated with the speed voltages divided by the shaft speed in mechanical radians per second.

Re-arranging this equation in terms of current and flux using equations 3, 5 and 6 in the  $\alpha$  and  $\beta$  reference frame, we can obtain:

$$T_E = \frac{3}{2}p_p \frac{L_M}{L_R}(\psi_{R\alpha}i_{S\beta} - \psi_{R\beta}i_{S\alpha}) \quad (1.24)$$

#### 1.1.2.4 Acceleration equation.

The electromagnetic torque developed by the motor drives the mechanical load. A mismatch between the electromagnetic  $T_E$  and mechanical  $T_L$  torques called differential torque accelerates the rotor mass. This can be expressed as:

$$T_E - T_L = J \frac{d\omega_m}{dt} = J \frac{d^2\theta}{dt^2} \quad (1.25)$$

Where  $\omega_m$  is the angular velocity of the rotor in radians per second and  $J$  is the polar moment of inertia of the rotor and the connected load. The load torque varies with the speed.

## Chapter 2 Field Oriented Control Strategies

Depending on the applications, control schemes for induction machines can be divided into two main groups: scalar and vector controls. The scalar control is based on using a frequency converter to regulate supply frequency of the machine. It is based on the steady-state model of the IM and therefore permits regulating at steady-state only the magnitudes and frequency of the stator voltages, currents, flux linkages, and electromagnetic torque. Many practical tasks can be carried out using scalar-controlled IMs. For example, they are ideal for pump and fan applications that do not call for accurate and highly dynamic torque control. Since it does not act on the angular position of the space vectors of the control variables, it does not permit the best dynamic performance to be achieved.

For more demanding applications, a more-sophisticated electrical drive control system is needed that monitors the electromagnetic state of the motor to more accurately manage torque.

Most of the control strategies are based on Vector control which is based on the dynamic model of the machine. They permit the drive to achieve its best dynamic performance in terms of electromagnetic torque control, thanks to their feature to take into consideration the instantaneous angular position of the stator voltages, currents as well as of the flux linkages. Some of the most common control strategies are shown in figure 2.1. Most of them will be described in this section. [5]

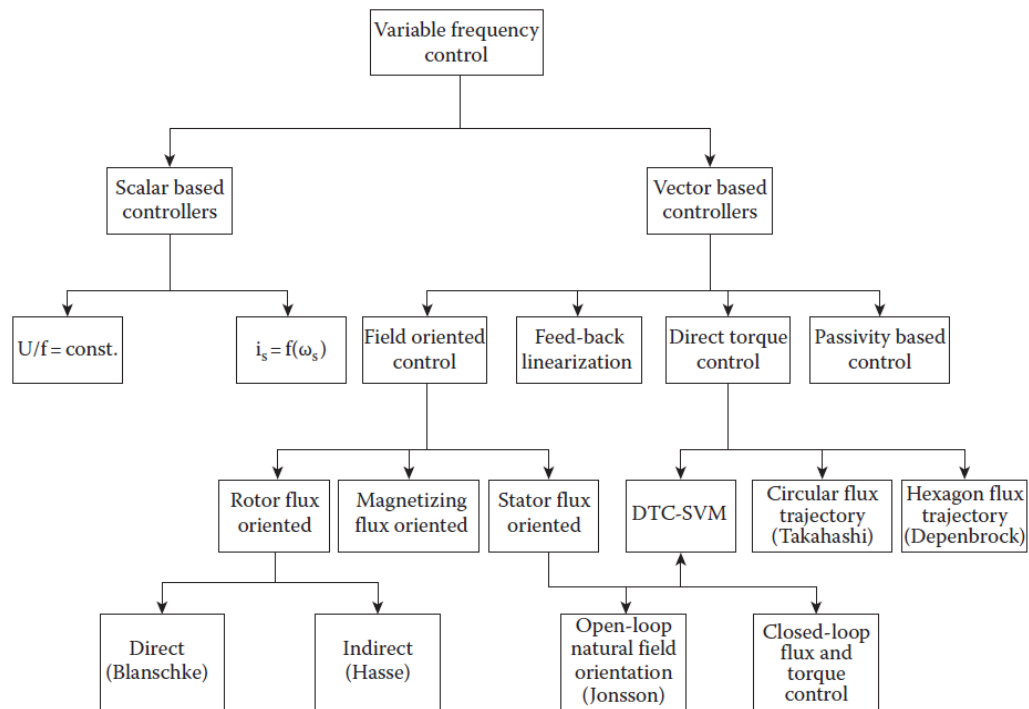


Figure 2-1 Induction Machine control classifications. [5]



## 2.1 Field Oriented Control.

Recently, AC machines have displaced DC machines as they require less maintenance and offer much higher power. However, the complicated dependence between flux linkage and torque control makes the control of AC machinery more difficult.

The most popular control method is well-known as **field-oriented control** (FOC), also called **vector control**, and has been proposed by Hasse and Blaschke. Although their concept has been improved over the time. The basic idea was always in the direction to develop a suitable coordinate transformation permitting the drive to be controlled in a decoupled way similarly with DC motor control, in other words, “make the IM behave as a DC machine”. A three-phase electric motor can be controlled using the complex space vector that represents all three of its phase quantities instead of designing three individual phase current controllers. [5]

Based on the space vector theory, if choosing a suitable rotating reference frame with the direct axis lying on the direction of the rotor, stator or magnetization flux-linkage space-vector makes it possible to write the instantaneous value of the electromagnetic torque as the product of the amplitude of the rotor (or stator or magnetization) flux linkage and the quadrature component of the stator current expressed in the same reference frame. This method allows to control the machine in steady state and even during transients. [2]

The FOC or vector control can be also be divided into three categories according to the variable oriented: rotor flux, stator flux or magnetizing flux oriented. The approach is similar in all of them as the electric torque generated by the machine can be expressed as the product of the amplitude of the rotor (or stator or magnetization) flux linkage and the quadrature component of the stator current expressed in the same reference frame.

As we showed in the last section, the electromagnetic torque can be expressed in the following form:

$$T_e = \frac{3}{2} p |\psi_s| |i_s| \sin \gamma' \quad (2.1)$$

Where  $T_e$  is the absolute value of the electrical torque,  $p$  is the number of pole pairs,  $i_s$  is the stator current space vector,  $\psi_s$  is the space vector for stator flux linkage, and  $\gamma'$  is the angle between the above two vectors. This equation is expressed in the stator reference frame but can also be expressed in the rotor or magnetization flux reference frames.

The equation 2.1 is similar to the electromagnetic torque equation of the DC motor with independent excitation. This indicates that the control of the electromagnetic torque should be performed, once the amplitude of the stator (rotor or magnetization) flux linkage amplitude is fixed, by acting on the quadrature components of the stator current space-vector in the chosen field reference frame.

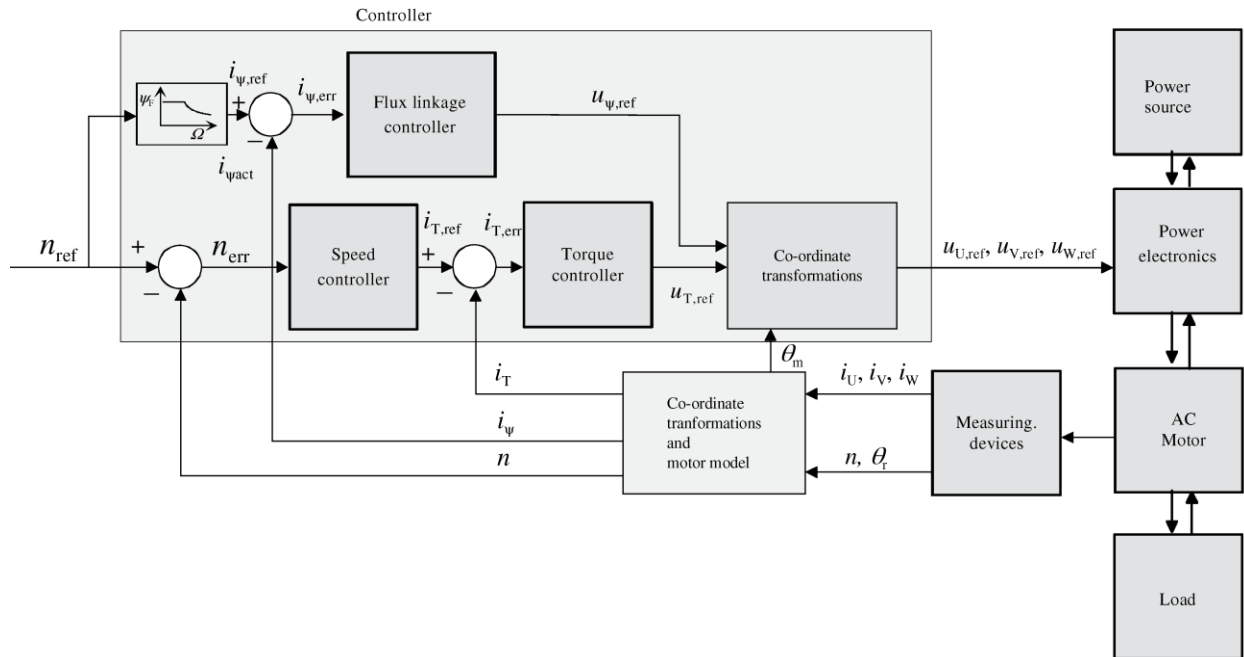


Figure 2-2 Scheme for the implementation of field-oriented control. [2]

Figure 2.2 shows a basic block diagram for the vector control. From this control diagram, we can observe that currents and speed should be measured. These currents are converted into the corresponding two-phase values. In the same block of conversion, we use the angle  $\theta_R$  to transform the currents to the rotational coordinate system (d-q). The flux linkage quantities can be obtained by measurements using Hall Effect sensors, but this usually means more expensive drives. Calculation based on the model's currents and voltages are used instead. The reference values for the currents and voltages used to control flux linkage and torque or force are calculated via PI controllers and realized in the air-gap flux-linkage aligned coordinate system. The reference values for the voltages that produce flux linkage and torque must be transferred to the stator coordinate system so they can be used by converter.

The IM will be fed through a PWM controlled VSI. The output of the control system is the value of the voltage that the inverter should generate. For this purpose, several PWM techniques could be used.

## 2.2 Direct Torque Control.

Direct Torque Control (DTC) is one of the most used electric drives control strategies. The strategy was developed by Takahashi and Depenbrock in the mid 1980's, but ABB has been the first and unique company to have introduced DTC controlled electrical drives since 1995. Like Field Oriented Control, in DTC it is possible to control the electric flux and electromagnetic torque of the machine in a decoupled and instantaneous way. [5][2]

This control strategy possess a simpler structure compared to the field-oriented control as it doesn't require PID controllers for motor flux and torque, no speed measurement, current and/or voltage decoupling network and two axis to three axis converter.

The control actions consists on tracking the references of magnetic flux and electromagnetic torque, by means of the application of suitable values of stator voltages of the machine. Since torque is the cross product of the space vector for stator flux linkage and the stator current space vector, the DTC only needs these two equations to realize ideal induction machine control. If the IM is supplied by a VSI, it is possible to control the stator flux linkage and electromagnetic torque by choosing the optimal switching configurations of the inverter. The VSI has eight switching states (six active and two zero states), which is obtained according 180° conduction mode. This optimal switching configurations should maintain the position of the stator flux linkage and electromagnetic torque inside hysteresis bands centered on relative reference values. With this we can obtain high dynamic performance in the torque response, low switching frequency of the inverter, and low losses due to the harmonics. [5][2]

DTC is implemented using the stator reference model, so no coordinate transformations should not be made. Also, stator flux linkage is controlled so this reduces the dependence of the motor parameters with the control efficiency.

### 2.2.1 Torque Expressions with Stator and Rotor Fluxes

The electromagnetic torque developed by an IM can be expressed as a function of the stator and rotor flux-linkage space-vectors as follows:

$$T_e = \frac{3}{2} \left( \frac{P}{2} \right) \boldsymbol{\psi}_s \mathbf{I}_s \quad (2.2)$$

If we represent flux and current vectors:

$$\boldsymbol{\psi}_s = \psi_{qs}^s - j\psi_{ds}^s \quad (2.3)$$

$$\mathbf{I}_s = i_{qs}^s - ji_{ds}^s \quad (2.4)$$

As we saw in the last section, fluxes can be expressed as function of currents:

$$\boldsymbol{\psi}_s = \mathbf{i}_s L_s + \mathbf{i}_r L_M \quad (2.5)$$

$$\boldsymbol{\psi}_r = \mathbf{i}_s L_M + \mathbf{i}_r L_R \quad (2.6)$$

If we express stator flux from equation 2.5 in terms of rotor flux:

$$\boldsymbol{\psi}_s = \frac{L_M}{L_R} \boldsymbol{\psi}_r + L'_S \mathbf{i}_s \quad (2.7)$$

Where  $L'_S = L_S L_R - L_M^2$  and the corresponding expression of  $\mathbf{i}_s$

$$\mathbf{i}_s = \frac{1}{L'_S} \boldsymbol{\psi}_s - \frac{L_M}{L_R L'_S} \boldsymbol{\psi}_r \quad (2.8)$$

Using this current expression into the torque expression:

$$T_e = \frac{3}{2} \left( \frac{P}{2} \right) \frac{L_M}{L_R L'_S} \boldsymbol{\psi}_r \boldsymbol{\psi}_s \quad (2.9)$$

The magnitude of torque is:

$$T_e = \frac{3}{2} \left( \frac{P}{2} \right) \frac{L_M}{L_R L'_S} |\boldsymbol{\psi}_r| |\boldsymbol{\psi}_s| \sin \gamma \quad (2.10)$$

Where:  $\gamma$  is the angle between the fluxes.

If we analyze this last equation, we can notice that it is possible to generate an instantaneous electromagnetic torque change by modifying the instantaneous angular position of the stator flux space vector. This variation is limited by the fact that the rotor flux-linkage space-vector tends to adapt itself to the variations of the stator flux-linkage space-vector. The angle  $\gamma$  between the two space-vectors tends to become zero in time. [5][2]

This equation justifies the fundamental premise of DTC, which is controlling stator flux linkage directly. We can consider that the rotor flux linkage  $\boldsymbol{\psi}_r$  is stable and rotates steadily.

### 2.2.2 Control Scheme.

Figure 2.3 shows a resumed schematic of the DTC control strategy. We can see that only two motor currents could be measured and the DC link voltage from the converter. No rotor position should be measured or calculated. The phase voltages and currents information is fed to the converter including the position of the switching. The motor model gives estimate values for torque, flux linkage, and rotation speed. The optimal switching logic selects optimum instantaneous switch positions based on torque and the state of the flux linkage.

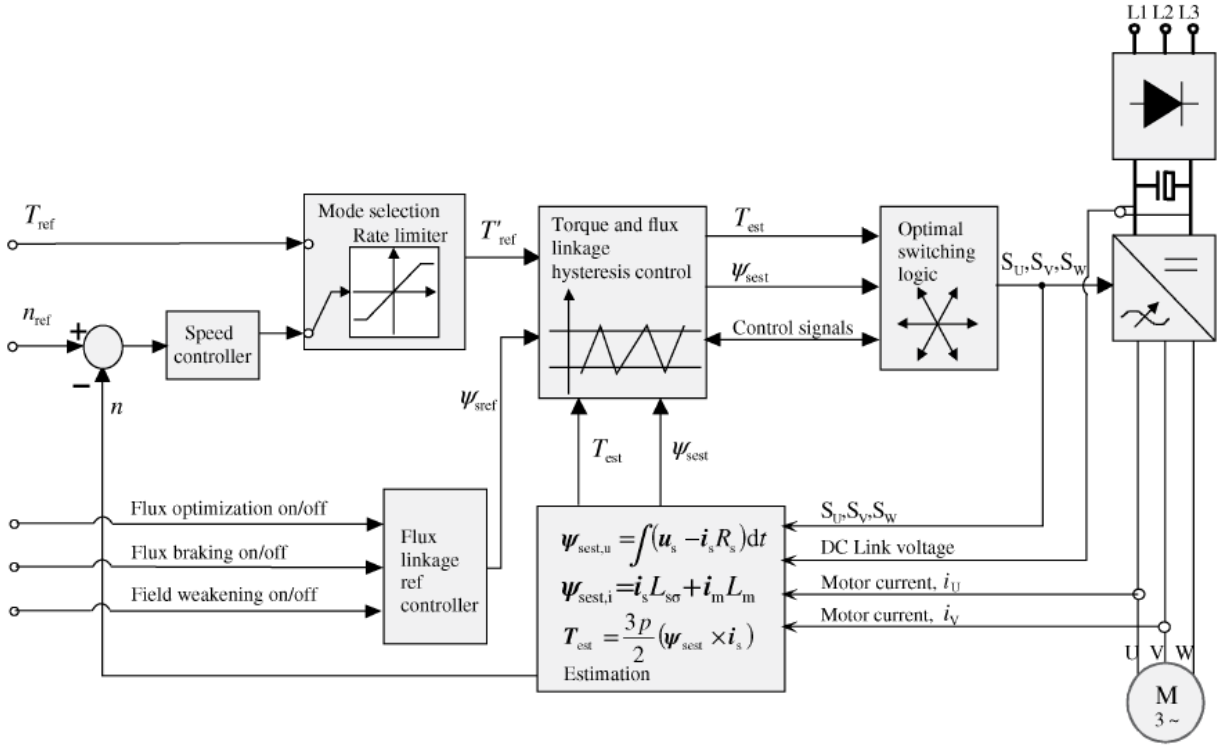


Figure 2-3 Direct Torque Control basic scheme. [2]

### 2.2.3 Control Strategy

As described before, the main criteria for this control strategy is the selection of the of the most suitable voltage vector at each sampling time of the control system. This voltage vector to be applied depends on the instantaneous angular position of the stator flux-linkage space-vector. The task of the control system is the selection of the most suitable voltage space-vector that permits modifying both: the amplitude and the angular position of the stator flux vector in the desired way.

The stator flux linkage can be estimated in the integral form of the flux equation:

$$\psi_{sest} = \int (\mathbf{u}_s - R_s \mathbf{i}_s) dt \quad (2.11)$$

Where;  $\mathbf{u}_s$  is the stator voltage space vector,  $R_s$  is the stator resistance in  $\Omega$  and  $\mathbf{i}_s$  is the stator current. All quantities can be calculated from measured voltages and currents. The term  $R_s \mathbf{i}_s$  is usually neglected and it weakens the stator flux. The stator voltage is then expressed in terms of the logic command signals to the upper devices of the inverter to obtain the relationship between the space-vector of the variation of the stator flux linkage and the inverter state configurations.

$$\psi_{sest} = \int (\mathbf{u}_s(S_a, S_b, S_c) - R_s \mathbf{i}_s) dt \quad (2.12)$$

In this case  $S_a, S_b$  and  $S_c$  correspond to the three converters witching functions, which receive values between 0 and 1 but usually just 0 and 1 are considered. If we also consider that the speed of the flux-linkage change is proportional to the DC-link voltage  $U_d$  and apply the definition of the space vector, we obtain:

$$u_s(t) = \frac{2}{3} U_d [a^0 S_a(t) + a S_b(t) + a^2 S_c(t)] \quad (2.13)$$

With this expression we can obtain six space vector configurations and if we add two zero vectors configurations, we can rotate the stator flux-linkage vector almost along a circular path. The path become more and more circular with increasing switching frequency.

Then it is necessary to ideally divide the complex plane on which the voltage and fluxes space-vectors lie into sectors of amplitude  $\pi/3$  ( $k=1$  through 6), each centered on one of the nonnull voltage space-vectors. We can see this configuration in figure 2.4. In each sector, two voltage vectors can be used in both rotation directions. One vector increases and the other decreases stator flux linkage. This control method require some hysteresis comparators to keep the stator flux vector and torque in given ranges. When the hysteresis limit is reached, the next suitable voltage vector is selected that will bring the stator flux-linkage vector to the right orientation. [5][2]

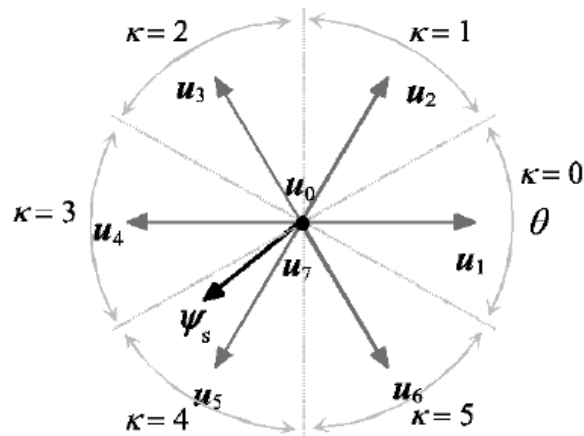


Figure 2-4 Flux-linkage circle division into sectors  $\kappa$  determined by the voltage vectors. [2]

Based on this thematic, Takahashi & Noguchi developed an optimal switching table by combining the hysteresis controls for flux linkage and torque with the position information of the flux-linkage vector. The vector combination is showed in image 2.5

Instantaneous Flux-Linkage Vector Location Sector							
Torque Bit $\tau$	Flux Linkage Bit $\phi$	$\kappa=0$	$\kappa=1$	$\kappa=2$	$\kappa=3$	$\kappa=4$	$\kappa=5$
-1	0	$u_5$	$u_6$	$u_1$	$u_2$	$u_3$	$u_4$
	1	$u_6$	$u_1$	$u_2$	$u_3$	$u_4$	$u_5$
1	0	$u_3$	$u_4$	$u_5$	$u_6$	$u_1$	$u_2$
	1	$u_2$	$u_3$	$u_4$	$u_5$	$u_6$	$u_1$
0	0	$u_0$ OR $u_7^*$	$u_0$ OR $u_7$	$u_0$ OR $u_7$	$u_0$ OR $u_7$	$u_0$ OR $u_7$	$u_0$ OR $u_7$

Figure 2-5 Optimal Switching Table. [2]

### 2.3 Feedback Linearization.

This control based implements a space of state model of the IM. Feedback linearization is a technique for analysis and design of nonlinear systems. The central idea of this approach is to algebraically transform the nonlinear system dynamics into a fully or partially linearized system so that the feedback control techniques could be applied. Marino have proposed a nonlinear transformation of the motor state variables so that, in the new coordinates, the speed and rotor flux amplitude can be decoupled by feedback; the method is called feedback linearization control (FLC) or input–output decoupling. [5]

### 2.4 Passivity Based Control.

A different possible approach, called passivity-based control (PBC), is based on the variation theory and energy shaping and has been focused recently. For this approach, the machine is modeled in terms of the Euler–Lagrange equations in generalized coordinates. [5]

## Chapter 3 Simulink Model

For our implementation we will use the equations described in chapter one to model the induction machine and these equations will be developed in Simulink. After we obtain our IM machine model, we then proceed to apply the field-oriented control strategy.

Machine parameters were taken from a real induction machine and will be detailed in the next section. As for the mathematical model of the induction machine, it is suggested you use the so-called “Stator Current – Rotor Flux Model” in a stator-fixed coordinate system ( $\omega_k = 0$ ). The real axis of this system is denoted as  $\alpha$  and the imaginary as  $\beta$ . The model is described by the set of differential equations described in coming sections.

### Induction Machine Parameters.

An induction machine from the laboratory was used for our simulation. This machine is designed to work with a supply from a standard three-phase voltage grid (line-to-line voltage 400 V, frequency 50 Hz). The machine is a real motor with the nameplate parameters as follows:

Parameter	Value
$P_n$	12 kW
$I_n$	22 A
$U_n$	400 V
$f_n$	50 Hz
$\cos\phi_n$	0.8
$n_n$	$1460 \text{ min}^{-1}$
$pp$	2

Table 1 Induction machine nameplate parameters.

Where:

- $P_n$  is the nominal machine power,
- $I_n$  is the nominal machine phase current (RMS),
- $U_n$  is the nominal machine line-to-line voltage (RMS),
- $f_n$  is the nominal machine supply frequency,
- $\cos\phi_n$  is the nominal machine power factor,
- $n_n$  is the nominal machine rotational speed, and
- $pp$  is the number of pole-pairs.



The electrical machine parameters that are used within its mathematical model have been obtained from the conventional no-load and lock-rotor tests. The moment of inertia has been measured from the motor deceleration characteristics:

Parameter	Value
$R_S$	0.370 $\Omega$
$R_R$	0.225 $\Omega$
$LS\sigma$	0.00227 H
$LR\sigma$	0.00227 H
$LM$	0.08 H
$LS$	0.08227 H
$LR$	0.08227 H
$J$	0.5 kg·m <sup>2</sup>

Table 2 Induction machine T-equivalent circuit parameters.

The machine parameters are very important for the control effectiveness. Very inaccurate measurements of inductances or resistances will translate into wrong control actions.

### 3.1 Equations for modeling IM.

For our induction machine model, we will use a stator fixed coordinate system. With this assumption, we can set the electrical angular speed  $\omega_k$  equals 0. For the machine model, equations in the Clarke transform will be used so  $\alpha$  for the real part and  $\beta$  for the imaginary one. The Stator Current – Rotor Flux Model will be implemented then the set of equations describing the machine should be the stator current and rotor flux variables.

We can start using equations 9, 19 and 20 to derive an equation relating the stator current and the rotor flux in  $\alpha$  coordinates:

$$u_{s\alpha} = R_S i_{s\alpha} + \sigma L_S \frac{di_{s\alpha}}{dt} + \frac{L_M}{L_R} \frac{d\psi_{R\alpha}}{dt} \quad (3.1)$$

Where  $\sigma$  is the leakage factor defined as  $\sigma = 1 - LM^2 / (LS \cdot LR)$ . Stator voltage will be used as an input in our model and stator current as our output. Rearranging this equation, we obtain:

$$\frac{di_{s\alpha}}{dt} = \frac{1}{\sigma L_S} \left( u_{s\alpha} - R_S i_{s\alpha} - \frac{L_M}{L_R} \frac{d\psi_{R\alpha}}{dt} \right) \quad (3.2)$$

Similarly, we can determine this expression for  $\beta$  coordinate:

$$u_{s\beta} = R_S i_{s\beta} + \sigma L_S \frac{di_{s\beta}}{dt} + \frac{L_M}{L_R} \frac{d\psi_{R\beta}}{dt} \quad (3.3)$$

And rearranging.

$$\frac{di_{s\beta}}{dt} = \frac{1}{\sigma L_S} \left( u_{s\beta} - R_S i_{s\beta} - \frac{L_M}{L_R} \frac{d\psi_{R\beta}}{dt} \right) \quad (3.4)$$

Given the amount of state variables and equations, we need two more equations to obtain a complete model of the machine. For this, we can use equations 14 and 15 for rotor voltage expressions in  $\alpha$ - $\beta$ .

The machine in question is a squirrel cage IM so the rotor voltage  $u_r = 0$ . Considering this, and in the same way as before, we obtain an equation relating stator current and rotor flux linkage. We then obtain:

$$\frac{d\psi_{R\alpha}}{dt} = \frac{R_R L_M}{L_R} i_{s\alpha} - \frac{R_R}{L_R} \psi_{R\alpha} - \omega \psi_{R\beta} \quad (3.5)$$

We can see that this expression contains the rotor-flux linkage with a term related to the angular velocity. This is because for our model we are considering a stator fixed reference frame, so there is a speed related flux linkage. The same expression for the  $\beta$  axis:

$$\frac{d\psi_{R\beta}}{dt} = \frac{R_R L_M}{L_R} i_{s\beta} - \frac{R_R}{L_R} \psi_{R\beta} - \omega \psi_{R\alpha} \quad (3.6)$$

Summarizing, the equations for the model:

$$\frac{di_{s\alpha}}{dt} = \frac{1}{\sigma L_S} \left( u_{s\alpha} - R_S i_{s\alpha} - \frac{L_M}{L_R} \frac{d\psi_{R\alpha}}{dt} \right) \quad (3.7)$$

$$\frac{di_{s\beta}}{dt} = \frac{1}{\sigma L_S} \left( u_{s\beta} - R_S i_{s\beta} - \frac{L_M}{L_R} \frac{d\psi_{R\beta}}{dt} \right) \quad (3.8)$$

$$\frac{d\psi_{R\alpha}}{dt} = \frac{R_R L_M}{L_R} i_{s\alpha} - \frac{R_R}{L_R} \psi_{R\alpha} - \omega \psi_{R\beta} \quad (3.9)$$

$$\frac{d\psi_{R\beta}}{dt} = \frac{R_R L_M}{L_R} i_{s\beta} - \frac{R_R}{L_R} \psi_{R\beta} - \omega \psi_{R\alpha} \quad (3.10)$$

$$T_E = \frac{3}{2} p_p \frac{L_M}{L_R} (\psi_{R\alpha} i_{s\beta} - \psi_{R\beta} i_{s\alpha}) \quad (3.11)$$

$$T_E - T_L = J \frac{d\omega_m}{dt} \quad (3.12)$$

$$\omega = p_p \omega_m \quad (3.13)$$

Where:

- $i_{S\alpha}$  and  $i_{S\beta}$  are components of the stator current space vector,
- $\Psi_{R\alpha}$  and  $\Psi_{R\beta}$  are components of the rotor flux linkage space vector,
- $u_{S\alpha}$  and  $u_{S\beta}$  are components of the stator voltage space vector,
- $\sigma$  is leakage factor defined as  $\sigma=1-L_{M2}/(L_S \cdot L_R)$ ,
- $T_E$  is the motor inner electromechanical torque  $T_l$  is the load torque,
- $J$  is the motor moment of inertia and
- $\omega_m$  is the rotor mechanical angular speed

The Torque equations are needed to emulate the dynamics of the machine load. The equations showed above, were implemented in Simulink to verify the behavior of the model. After the correct implementation, the control scheme will be developed and afterward the simulation in dSpace will take place.

### 3.2 Simulink model of the IM.

For the implementation of our model, equations from 3.7 to 3.13 will be used. The method for this will be basic blocks from the Simulink library.

The given model consists of the  $\alpha$  and  $\beta$  components (or Clarke transformation) of the currents and flux linkages. This implies that the input voltages should be transformed to its  $\alpha$  and  $\beta$  components as well. For this this task, the blocks shown in figure 3.1 where used. In practice, this input signals are given by a power converter like a VSI.

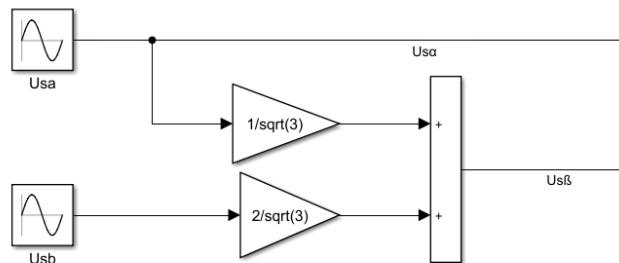


Figure 3-1  $\alpha$  and  $\beta$  components of supply voltage.

Where:

$$U_{Sa} = \frac{U_n}{\sqrt{3}} \cos \omega_s t$$

$$U_{Sb} = \frac{U_n}{\sqrt{3}} \cos(\omega_s t - \frac{2\pi}{3})$$

And the transformed voltages:

$$U_{S\alpha} = U_{Sa} \text{ and } U_{S\beta} = \frac{1}{\sqrt{3}}U_{Sa} + \frac{2}{\sqrt{3}}U_{Sb}$$

The voltages  $U_{S\alpha}$  and  $U_{S\beta}$  will be the input voltages for our model. The resulting Simulink model will be shown by parts.

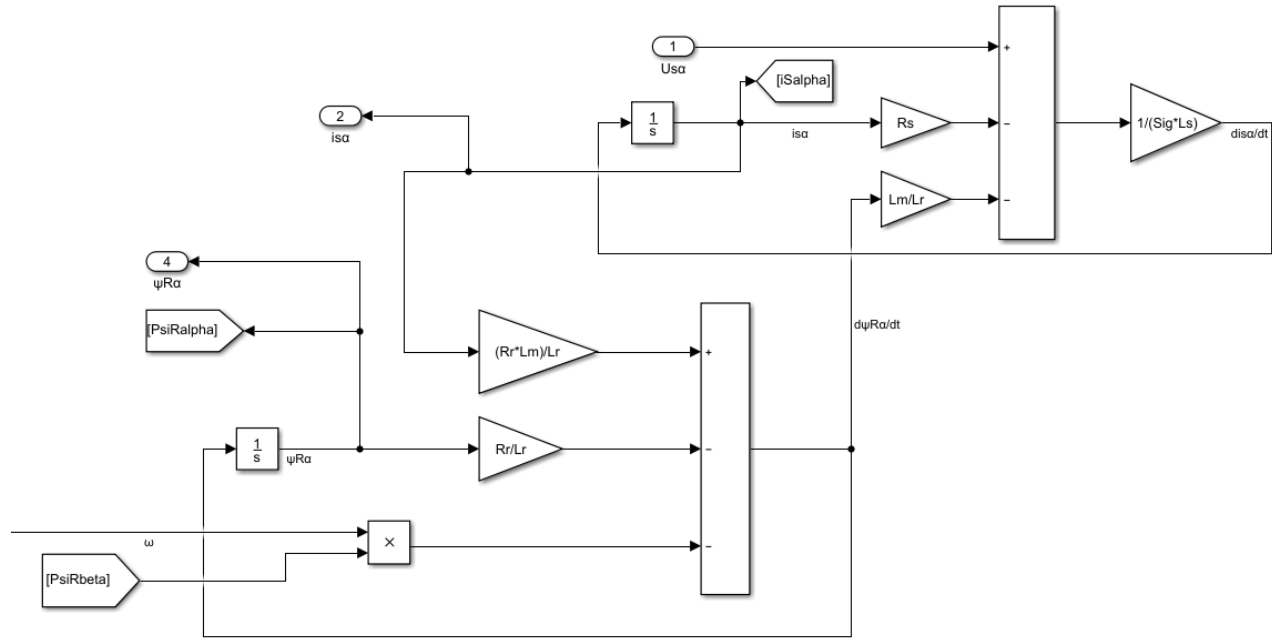


Figure 3-2 Modelling for  $i_{S\alpha}$  and  $\psi_{R\alpha}$ .

Figure 3.2 shows the model for the equations describing current  $i_{S\alpha}$  and flux linkage  $\psi_{R\alpha}$ . The voltage  $U_{S\alpha}$  is input and the two mentioned variables are output for our analysis. The angular

velocity  $\omega$  model will be shown later.

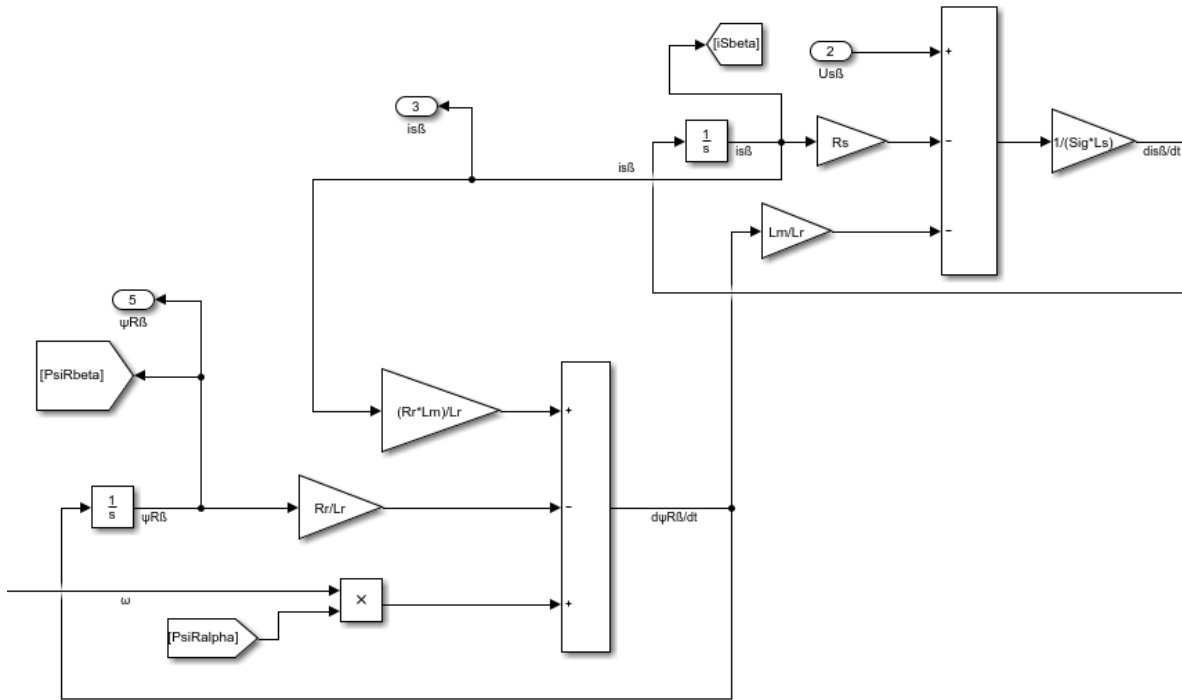


Figure 3-3 Modelling for  $i_{S\beta}$  and  $\psi_{R\beta}$ .

The image 3.3 shows the model for current  $i_{S\beta}$  and flux linkage  $\psi_{R\beta}$ . This is the same model as for  $i_{S\alpha}$  and  $\psi_{R\alpha}$ . In this case voltage  $U_{S\beta}$  is the input.

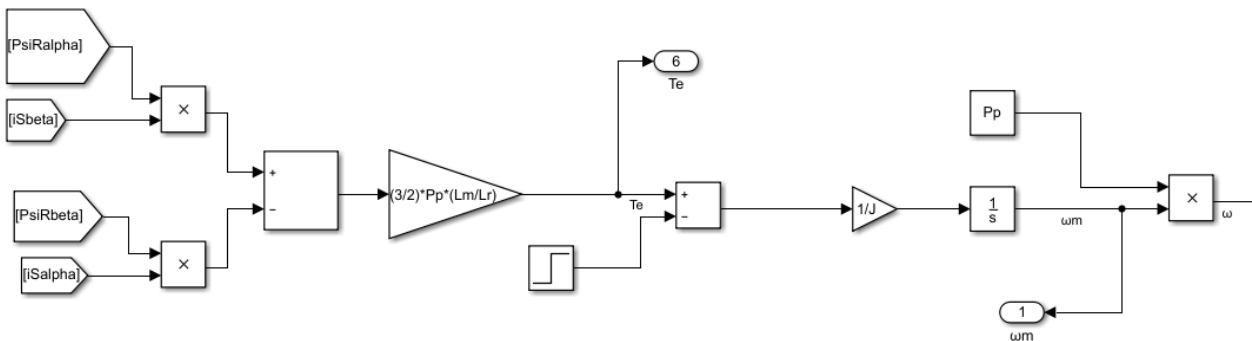


Figure 3-4 Modelling of torque and speed section.

The picture above shows the Torque-Speed part of the model. Electric torque is dependent of the currents  $i_{S\beta}$  and  $i_{S\alpha}$  and flux linkages  $\psi_{R\alpha}$  and  $\psi_{R\beta}$ . The equation describing  $T_E$  is represented in the integral form.

All the previous showed blocks can be represented by subsystems for simplification. The resulting system is shown in figure 3.5.

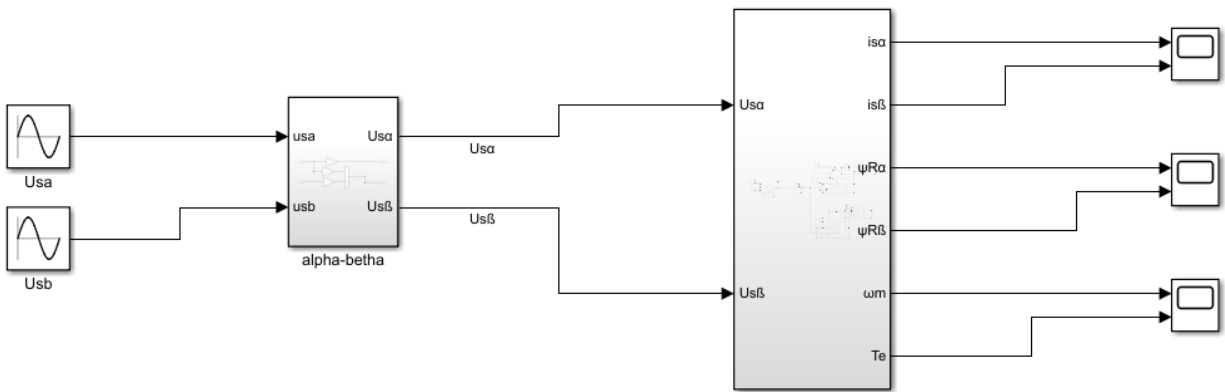


Figure 3-5 Complete IM model.

### 3.4 Field Oriented Control.

Our next task consist on implementing a field-oriented control strategy to our IM. For the Field Oriented control scheme, we must control the  $d$  and  $q$  components of the current. So, a coordinate transformation must be built. The block is shown in figure 3.6.

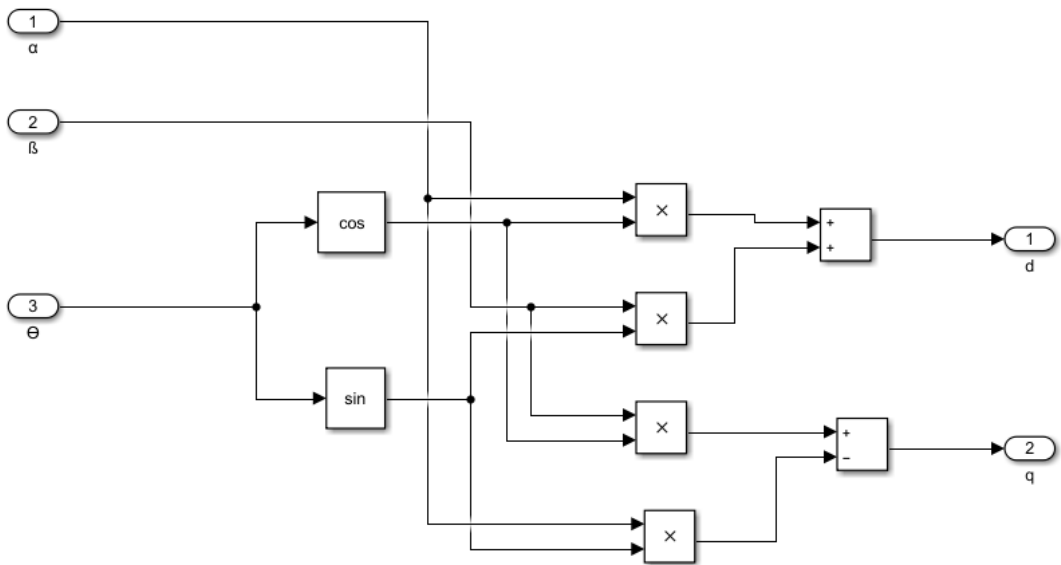


Figure 3-6  $\alpha$ - $\beta$  to  $d$ - $q$  transformation.

In this block we can see that the  $\alpha$  and  $\beta$  and transformation angle  $\Theta$  are the inputs and the  $d$  –  $q$  quantities the outputs. For our specific model,  $i_{S\alpha}$  and  $i_{S\beta}$  where transformed in  $i_{Sd}$  and  $i_{Sq}$ .

### 3.4.1 Flux Estimation.

It is quite simple to calculate stator flux linkage based on the integral form  $\psi_{Sest} = \int (\mathbf{u}_s - R_s \mathbf{i}_s) dt$  described in the previous chapter. With this equation, very accurate results can be obtained as only the stator resistance parameter of the machine is needed. Stator and rotor flux linkages can also be directly measured via Hall Effect sensors, but this option is regularly not used as the drive becomes more complex and expensive. Rotor flux linkage can also be calculated; however, more parameters of the machine should be determined, and the efficiency of the drive depends on the accuracy of this parameters. Image 3.7 shows a rotor flux linkage estimator based on the previous rotor flux equations. [10]

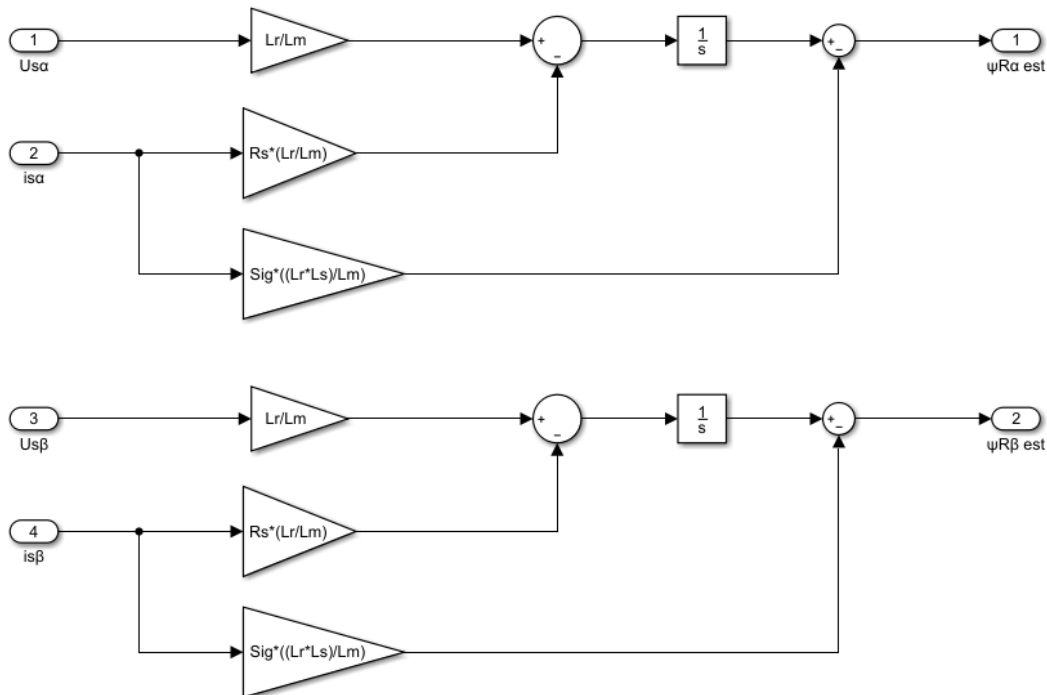


Figure 3-7 Rotor Flux estimation blocks.

The rotor fluxes could also be obtained directly from our IM model. But in this way, the control scheme can be implemented in a more independent or sensor less way.

### 3.4.2 Speed Estimator.

In recent years, attempts to remove the speed or position sensor in the shaft of induction machine (IM) drives with the intention to make it sensor-less or encoder-less. The main advantages of sensor-less-controlled drives are the reduced hardware complexity, the lower cost, the reduced size of the drive machine, the elimination of the sensor cables, the better noise immunity, the increased reliability, and the lower maintenance requirements. Various speed estimation techniques have been developed with different accuracies depending on the application of the drive.

A good alternative is a closed loop speed estimator, also called observers. We will implement a classic Model Reference Adaptive Systems or MRAS in our model. All the MRAS observers are based on the schematic of a reference model and an adaptive model. Some IM state variables are estimated at the same time with both the reference and the adaptive models; the difference between these two estimations is then processed by an adaptation mechanism, which gives the estimated speed by adjusting the adaptive model so that its output coincides with that of the reference model. The various MRAS schemes differ from one another by the chosen state variables.

A basic MRAS scheme using the rotor flux will be implemented. For our case, the reference model is described by the stator voltage equations in stator reference frame and the adaptive model is based on the rotor equations in the stator reference frame. The angular difference between both models is fed to a PI controller, which, should reduce the error between two models by aligning the adaptive model with the reference model. Both models are defined in the equations 3.14,3.15 and 3.16, 3.17. The diagram of the model is shown in image 3.8.

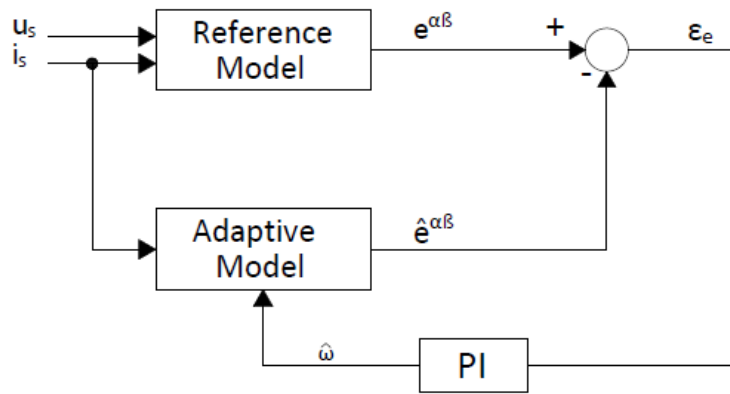


Figure 3-8 Speed Estimator general scheme.

Reference Model:

$$\frac{d\psi_{R\alpha}}{dt} = \left( u_{s\alpha} - R_s i_{s\alpha} - \sigma L_s \frac{di_{s\alpha}}{dt} \right) \quad (3.14)$$

$$\frac{d\psi_{R\beta}}{dt} = \left( u_{s\beta} - R_s i_{s\beta} - \sigma L_s \frac{di_{s\beta}}{dt} \right) \quad (3.15)$$

Adaptive Model:

$$\frac{d\hat{\psi}_{R\alpha}}{dt} = \frac{1}{\tau_r} (L_M i_{s\alpha} - \hat{\psi}_{R\alpha} - \omega \tau_r \hat{\psi}_{R\beta}) \quad (3.16)$$

$$\frac{d\hat{\psi}_{R\beta}}{dt} = \frac{1}{\tau_r} (L_M i_{s\beta} - \hat{\psi}_{R\beta} - \omega \tau_r \hat{\psi}_{R\alpha}) \quad (3.17)$$



Then, the speed is estimated in the following way:

$$\hat{\omega}_r = K_p(\psi_{R\beta}\hat{\psi}_{R\alpha} - \psi_{R\alpha}\hat{\psi}_{R\beta}) + K_i \int (\psi_{R\beta}\hat{\psi}_{R\alpha} - \psi_{R\alpha}\hat{\psi}_{R\beta})dt \quad (3.18)$$

Our Simulink model is presented below. We can verify that for our reference model we simply took the rotor flux estimator.

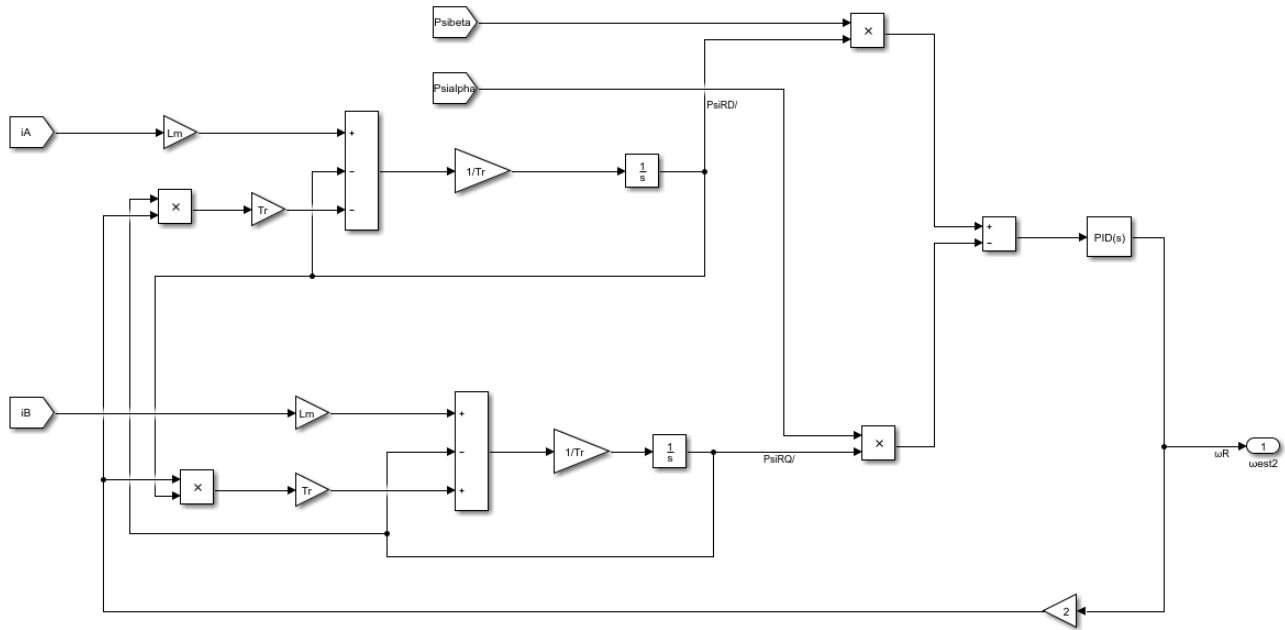


Figure 3-9 Speed Estimator Simulink model.

### 3.5 Full control scheme.

In figure 3.10 we can see the control scheme implemented in our model. The stator voltages are applied to the IM model in  $\alpha$ - $\beta$  coordinates. The flux reference  $\psi_{ref}$  is fixed to 1 Wb and the  $\omega_{ref}$  is our setting which we will input different variations such as ramps and steps to study the behavior of our control system. The variables will be controlled in the d-q reference frame so two transformation blocks are required. We can see that the rotor flux is estimated from the stator current and voltages and then used as the measured signals for our PI controllers. The speed estimator requires the stator current signals measured from the machine and the rotor flux calculated from the previously described block. This estimated speed is then used to determine the error signal used in the controller. We can see the relationship between the quadrature-axis current and the mechanical speed and the direct-axis current with the magnetizing flux of the machine.

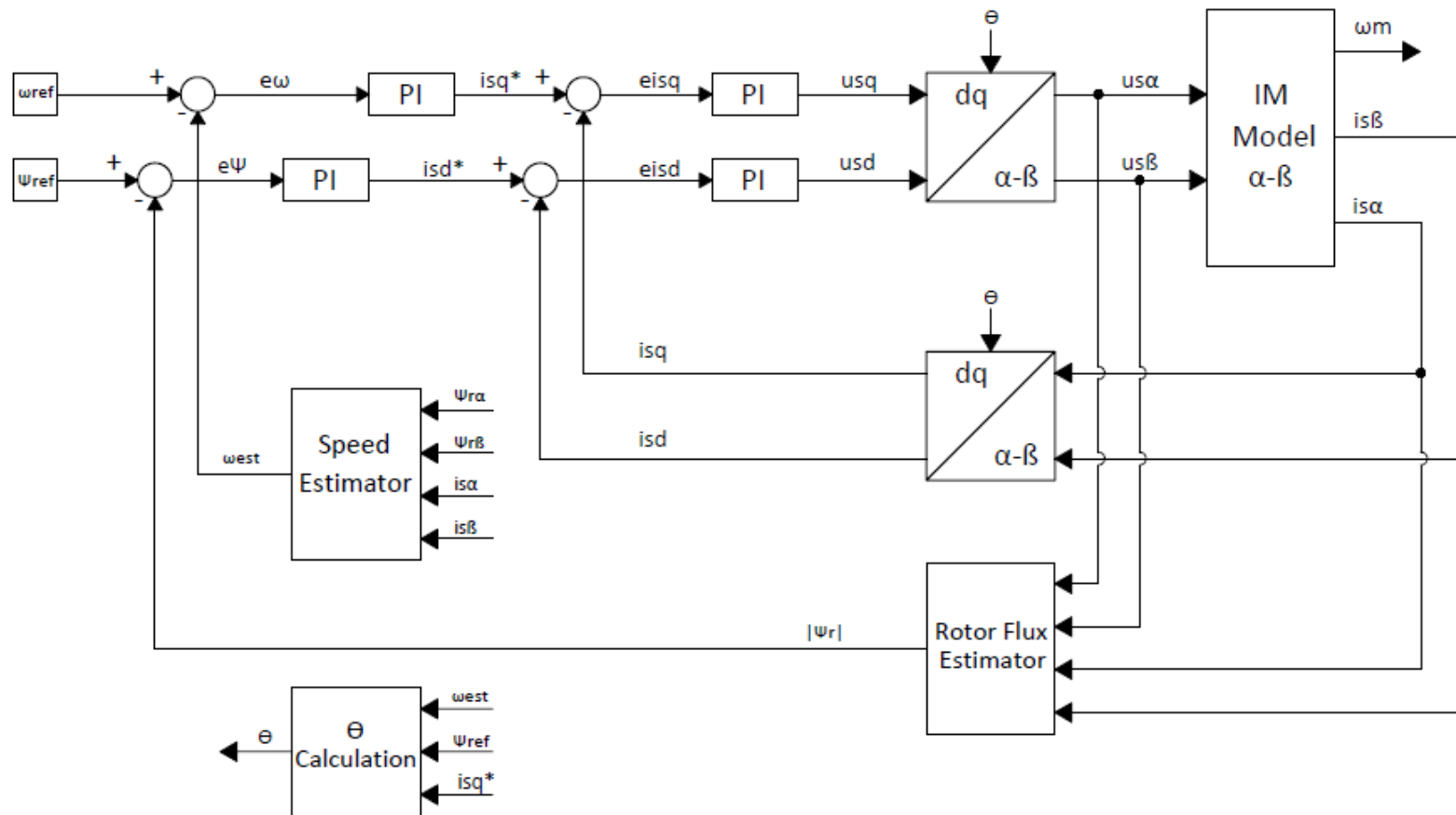


Figure 3-10 Implemented general control scheme.

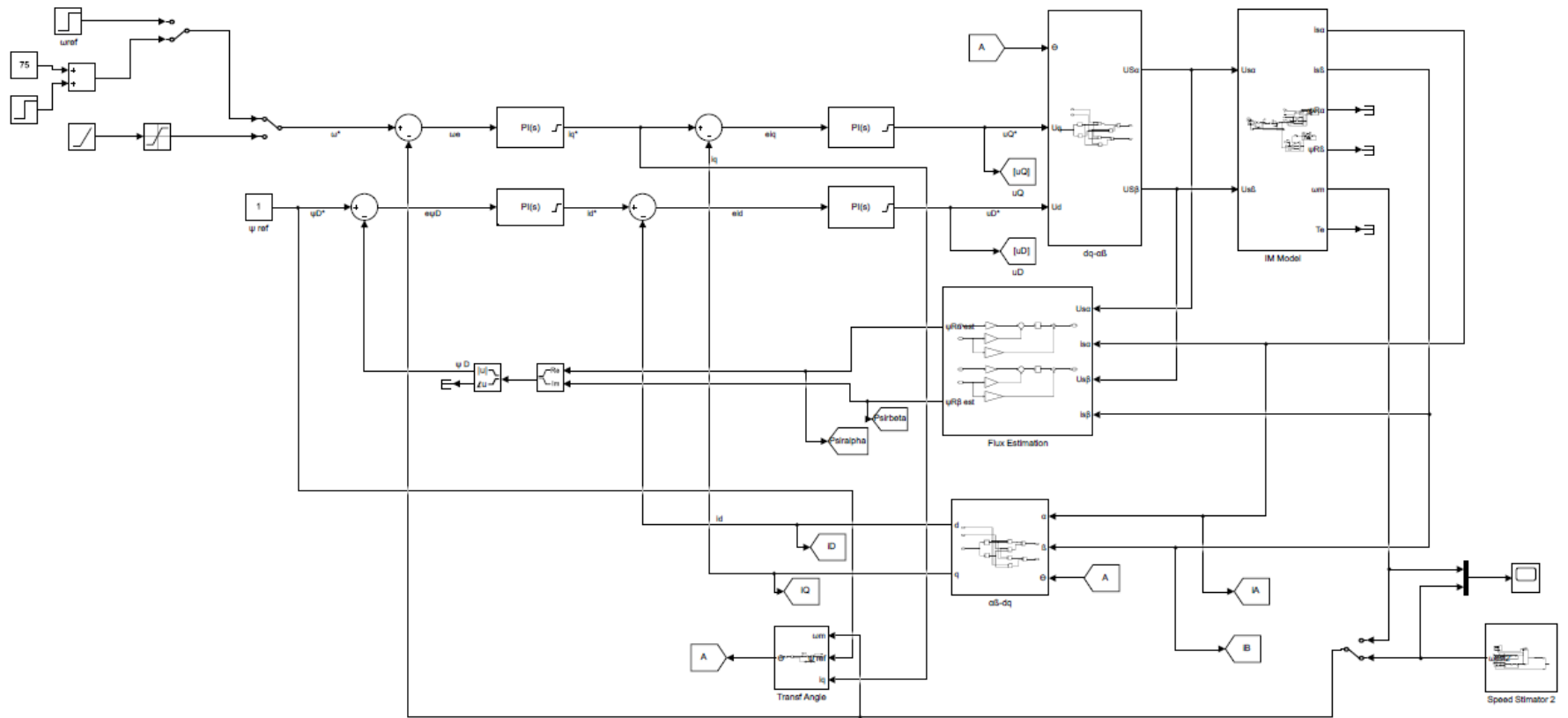


Figure 3-11 Full Simulink schematic.

### 3.6 Simulations.

The methodology to follow in our study consist in applying different speed reference signals and load torque to the model and verify the behavior of its controlled variables. The flux reference will be fixed to 1 Wb. The model is designed to work in a decoupled way so the speed quantity will be taken from the speed estimator.

The measured variables will be:

- Actual stator flux in d axis  $\psi_{sd}$  and reference flux  $\psi^*$  in Wb.
- Actual stator current in q axis  $i_{sq}$  and reference stator current in d axis  $i_{sd}^*$  in A.
- Induction machine measured speed  $\omega_m$ , estimated speed  $\omega_{est}$  and reference speed  $\omega^*$  in rad/sec.
- Load torque  $T_L$ , electromagnetic Torque  $T_e$  and Machine torque which is the difference between mentioned torques.

#### 3.6.1 Case 1: Constant speed, speed step and load step.

For our first simulation, with unloaded machine, we will apply a step with the nominal speed (153 rad/s approx.) at  $t = 2$  seconds and then apply a step load torque (78 Nm/s approx.) at  $t = 4$  seconds. The results will be shown in next images.

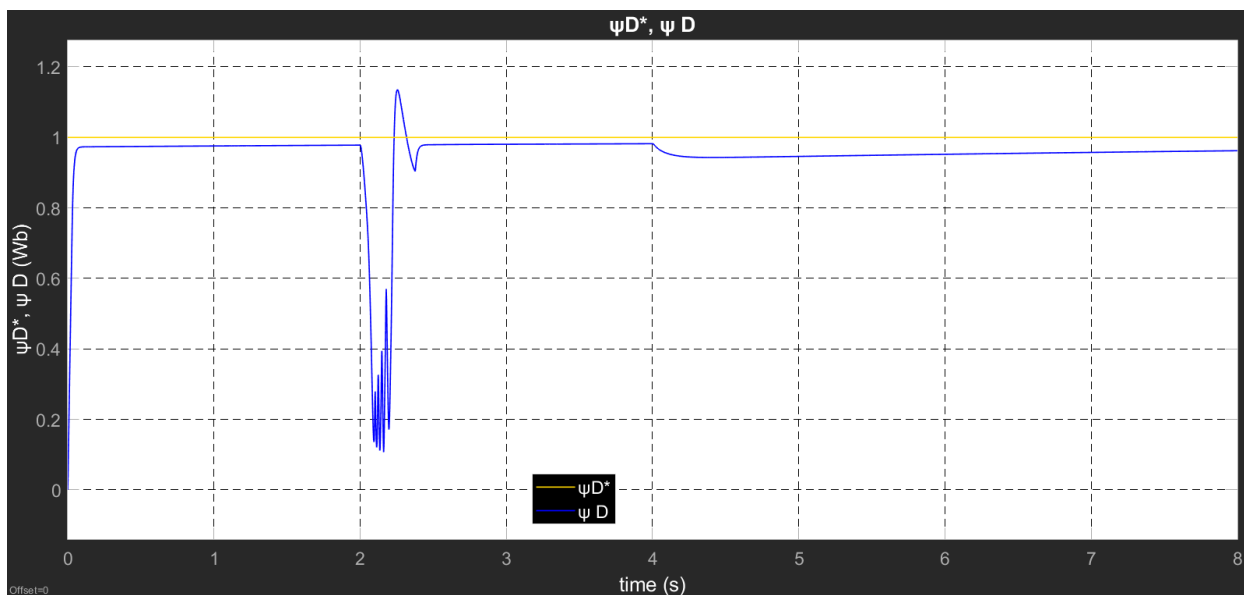


Figure 3-12 Reference and actual flux for case 1.

Figure 3.12 shows the behavior of the flux during both disturbances. At  $t=0$  s, the calculated flux starts almost like an impulse signal but stays around 0.975 Wb with a steady state error or 2.5%. When the speed step is applied in  $t=2$  s, we can see a considerable disturbance with its lowest peak reaching 0.1141 Wb and its highest peak 1.127 Wb with an overshoot of around 13 %. At  $t=4$  seconds, the load is applied, and the flux decreases slightly at a maximum lower peak of

0.9448 Wb and then starts to slowly increase to 0.9612 Wb. This behavior is normal as the load generates a field weakening which reduces the flux linkage in the stator of the machine.

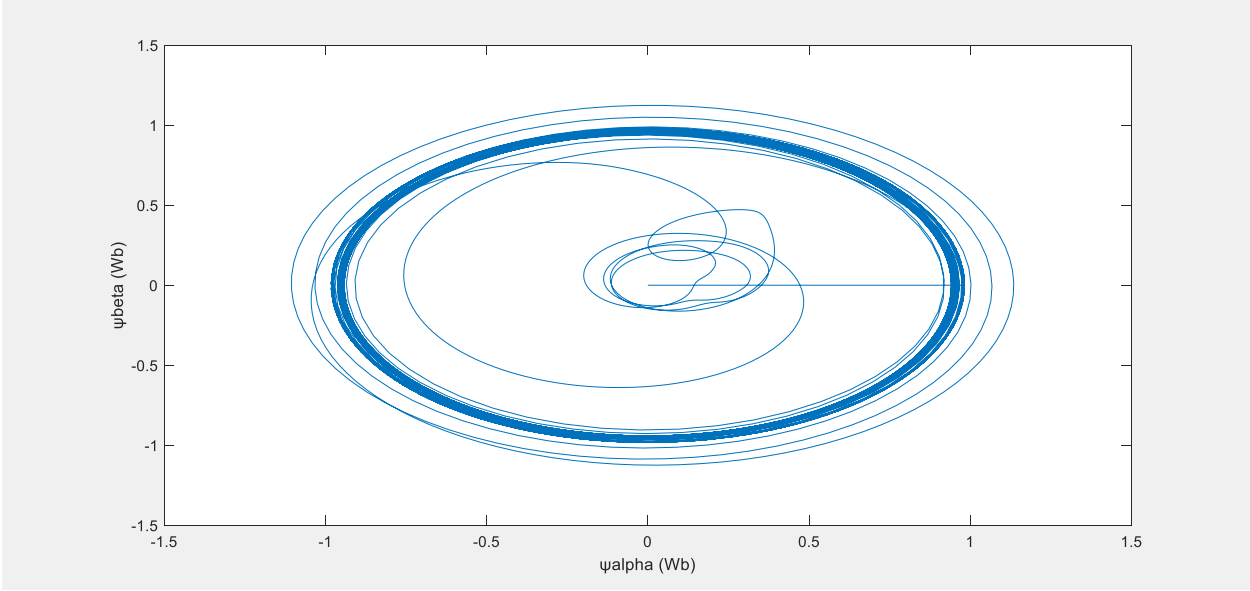


Figure 3-13 Flux in polar coordinates for case 1.

Figure 3.13 shows the flux in polar coordinates, we can see that the controller is doesn't keep the flux in a circular trajectory for the whole control interval, this is a consequence of the error during the speed estimation.

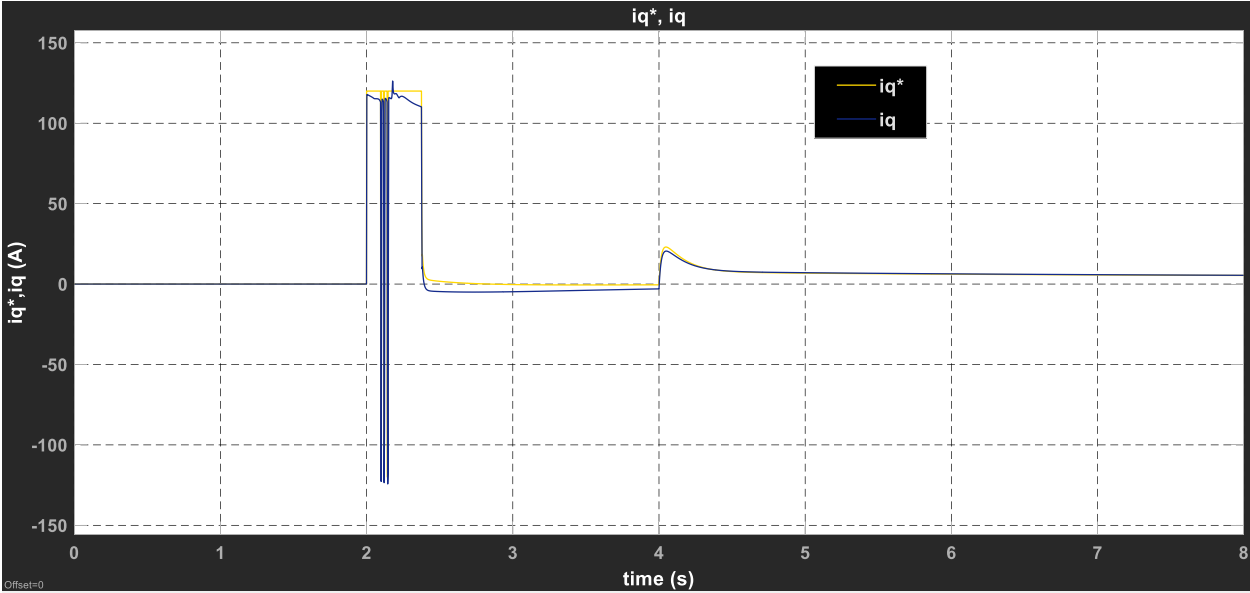


Figure 3-14 Reference and actual iq for case 1.

As it was mentioned in the previous chapter, the concept of field-oriented control is to control direct and quadrature currents. Quadrature current component controls the machine torque. In figure 3.13 we see the current is 0 in the machine startup as no mechanical load is applied. When the speed step is applied in  $t=2$  seconds, the current also reacts as a step with some oscillations, which means the machine is breaking the inertia so rotation can start. The actual current starts increasing slowly till almost reaching the 0 steady state value again at  $t=4$  s, in that moment the load torque is applied and there is a peak that reaches 23.04 A for the actual  $i_q$  and 20.48 A for the reference  $i_q$  with an error of approx. 12%. Both currents then reach the steady state of around 7A. Between 2.10 and 2.15 seconds, strong oscillations can be observed, both in reference an actual torque, the speed estimator shows having a considerable error during the calculations during a step change in speed.

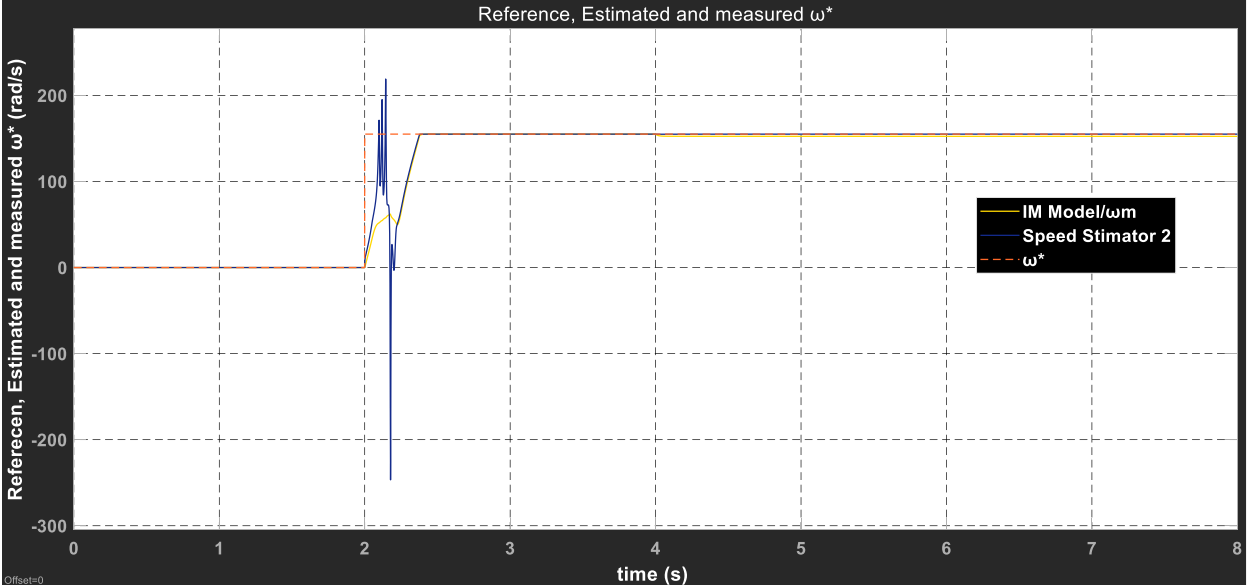


Figure 3-15 Machine, reference and Estimated Speeds for case 1.

The previous image 3.14 shows the reference, measured and estimated speeds. When the speed step is applied, the machine speed response is slow as it takes 0.413 seconds to reach the desired speed and shows a high and low peak before stability. On the other hand, the estimated speed shows higher and lower peaks and then become stable at the same time as measured speed. Note that when load is applied, the measured speed decreases slightly 2.7 rad/sec and both estimated and reference speeds are equal.

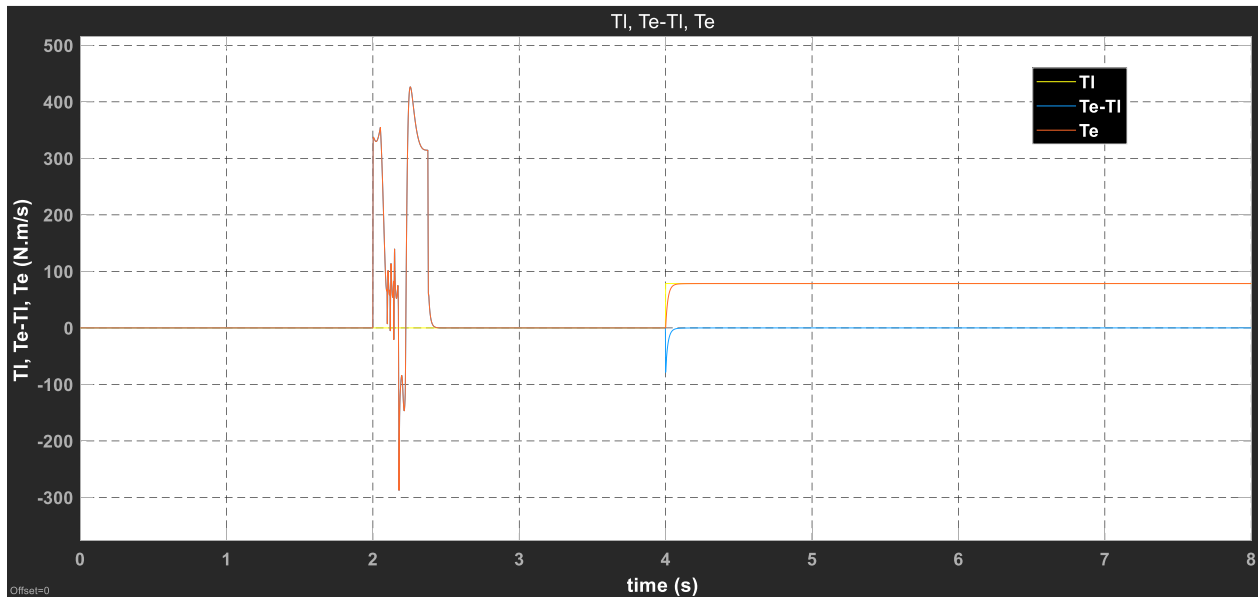


Figure 3-16 Load torque, Machine torque and Electromagnetic torque for case 1.

Figure 3.15 shows the different torque reactions for case 1 scenario. Initially, both; electromagnetic and IM machine torque are 0 as the machine is not running. When the step speed is applied, similar to  $i_q$ , some higher and lower peaks with oscillations are observed. The torque goes back to steady state after 0.42 seconds. Load is applied at  $t=4$  seconds and a brief acceleration torque is observed but then the system reaches its steady state. For the load step we obtained a desired response.

### 3.6.2 Case 2: Speed Ramp, constant speed, negative speed step and load torque step.

For case 2, as for the speed, a ramp was implemented, then, after nominal speed is reached around  $t=3.1$  seconds. A step is then applied where reference speed is decreased to 95 rad/s and is kept constant. In  $t=6$  seconds nominal load torque is then applied. The results will be shown in next images.

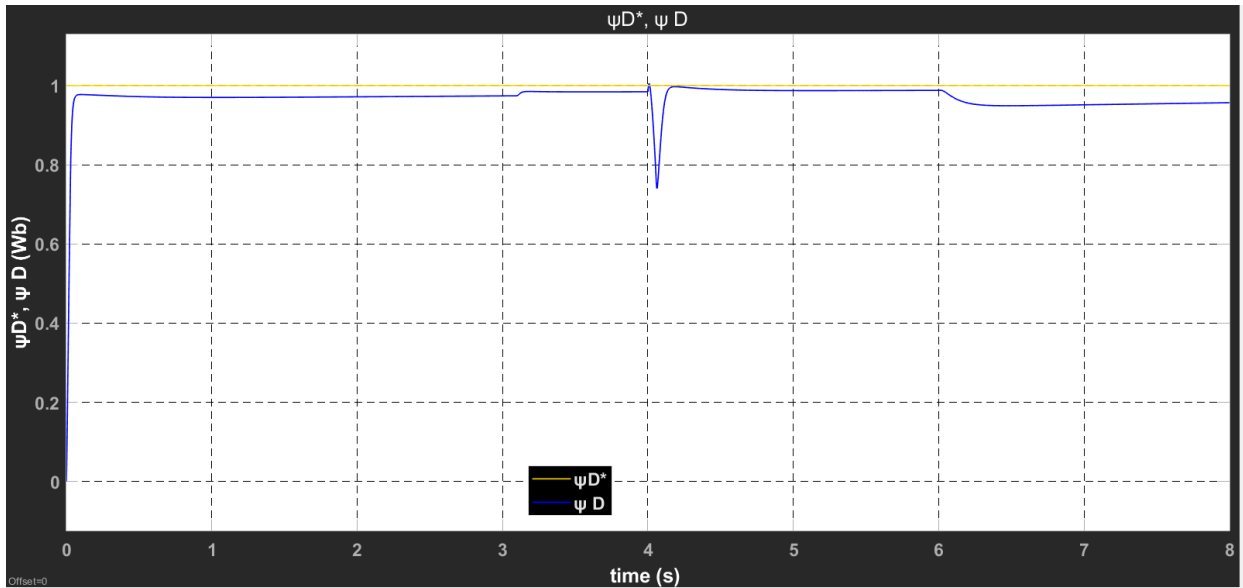


Figure 3-17 Reference and actual flux for case 2.

From the image above, we can see that the machine is quickly magnetized as flux reaches to 0.97 Wb. While the speed is increasing, the flux slightly decreases and increases steadily. As the machine reaches its nominal speed, the flux reaches its normal point at 0.98 Wb. When the speed step is applied, the flux reaches a low peak at 0.74 Wb and quickly reaches its steady state as the machine its demagnetized and then magnetized. After the load is applied, we can see that the machine is demagnetized as the flux reduces to around 0.95 Wb. The picture shows that the demagnetization of the machine is not attenuated by the lower speed.

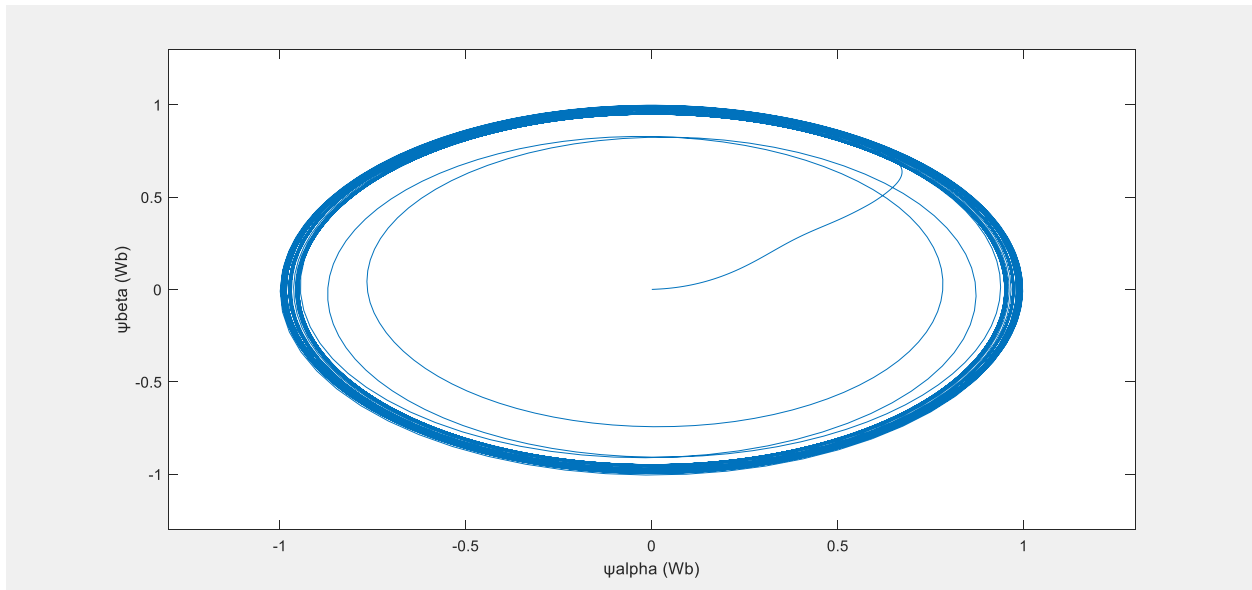


Figure 3-18 Flux in polar coordinates for case 2.



For this case we can also verify a better control behavior as the flux has a circular trajectory for most of the time lapse.

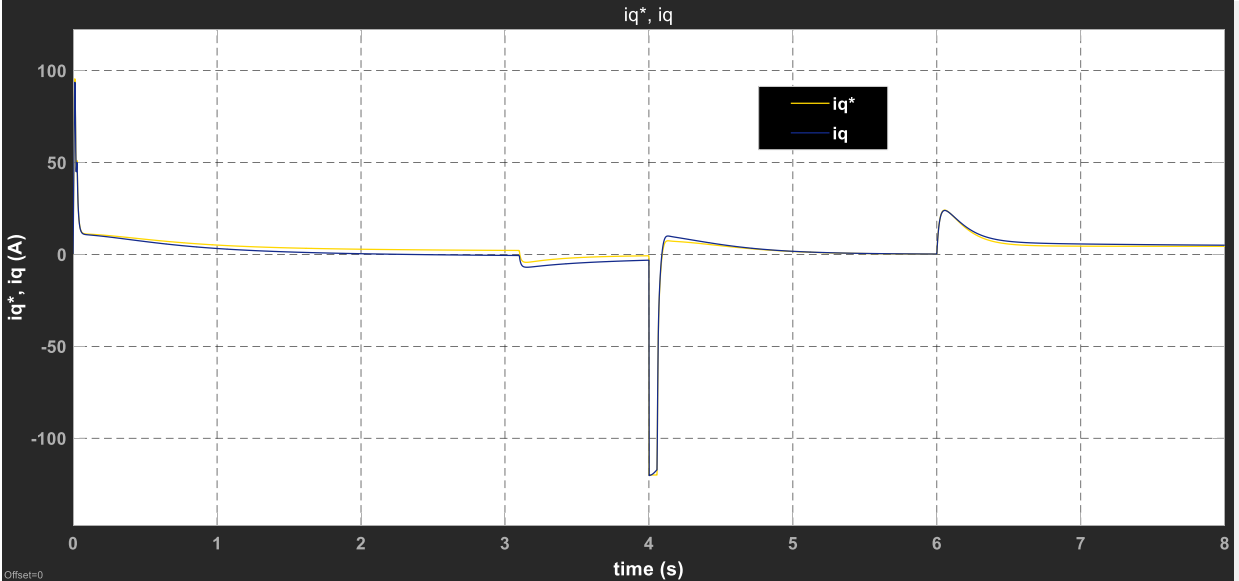


Figure 3-19 Reference and actual iq for case 2.

In this picture we see a more dynamic behavior of the iq. As iq is related to the electromagnetic torque of the machine, it is necessary to start pulling off the inertia. We can see a current peak at the start and then slowly decreases when reaching the nominal speed. Another slight step it seem at t=3.1 seconds as the machine is reaching a steady speed it is necessary a slight brake. When the speed step its applied, currents reach a low peak of 120 A, as it is necessary to brake abruptly to reduce from nominal speed to the new settled speed of 95 rad/s. When the load is applied, another current peak is observed as it is necessary to increase the quadrature current to increase the torque. The currents stabilizes at 7.1 A for the reference and 7.29 A to the measured currents. Notice the steady state error of approx. 2.1 % is positive in this case.

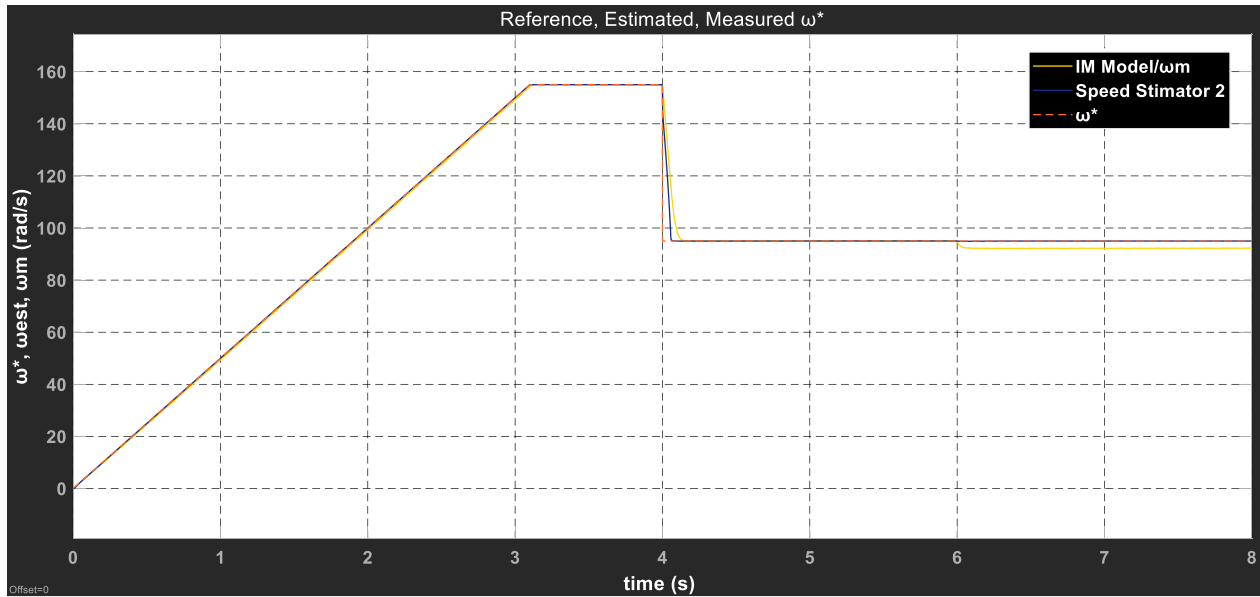


Figure 3-20 Machine, reference and Estimated Speeds for case 2.

In relation to the speed, graph in figure 3.18 shows machine, reference and estimated velocities. The variation is minimal in the whole simulation. We can see that the response of the speed estimator is very accurate in relation to the real measured speed. When negative speed step is reached in  $t = 4$  seconds, we can see that the response of the estimator is faster than the real speed. It is natural for this kind of systems to have a damped response. When the load is applied at  $t=6$  seconds, the small variation between measured and estimated persist of around 2.8 rad/s.

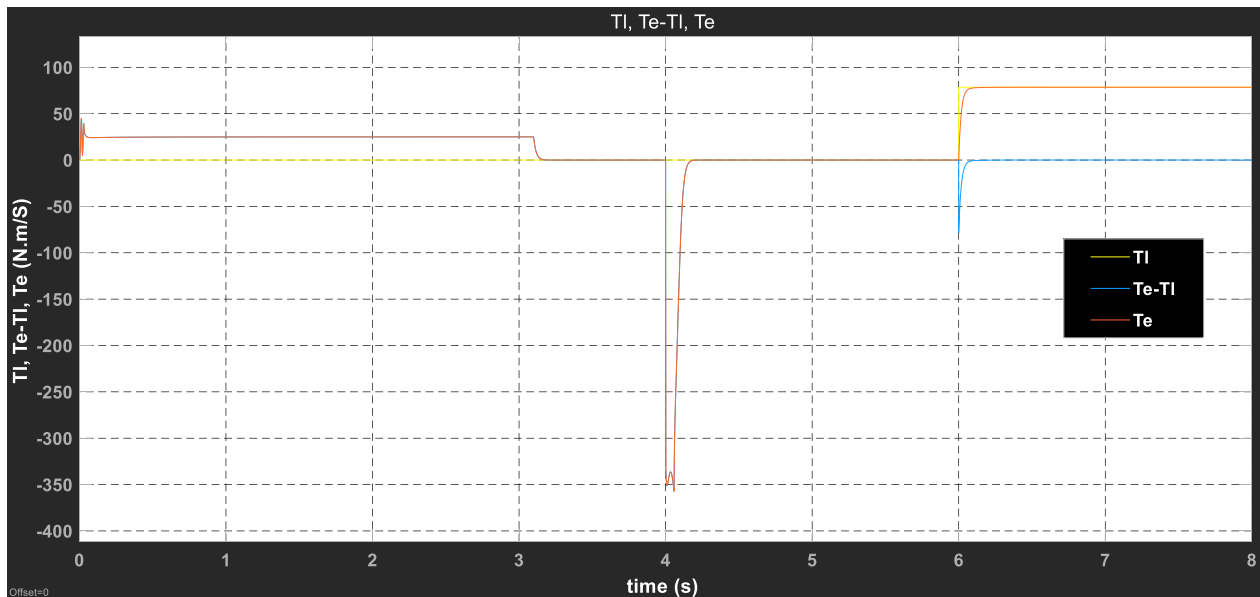


Figure 3-21 Load torque, Machine torque and Electromagnetic torque for case 2.

Figure 3.19 shows the relations for different torques. From  $t=0$  to  $t = 6$  seconds the machine is in no load regime but a constant electromagnetic torque of approx. 25 Nm/s is measured as the

machine is accelerated to reach nominal speed. When nominal speed is achieved, the  $T_e$  turns 0 as the machine is running at constant speed (no acceleration). When the speed negative step is applied, a short but high electromagnetic torque peak is measured as the machine should reduce speed abruptly reaching around 350 Nm/s and lasting around 0.18 seconds. The machine then goes back to steady state. When the load step is applied we can observe a negative peak on the acceleration torque and after it the machine works in steady state.

### 3.6.3 Case 3: Speed Estimator at lower speeds.

For the next case we want to analyze the behavior of the estimator for speed step at  $t=0$  and the behavior at low speeds. A speed ramp will be applied at  $t=3$  seconds till a speed of 3 rad/s is reached. At  $t=7$  seconds a nominal load will be applied.

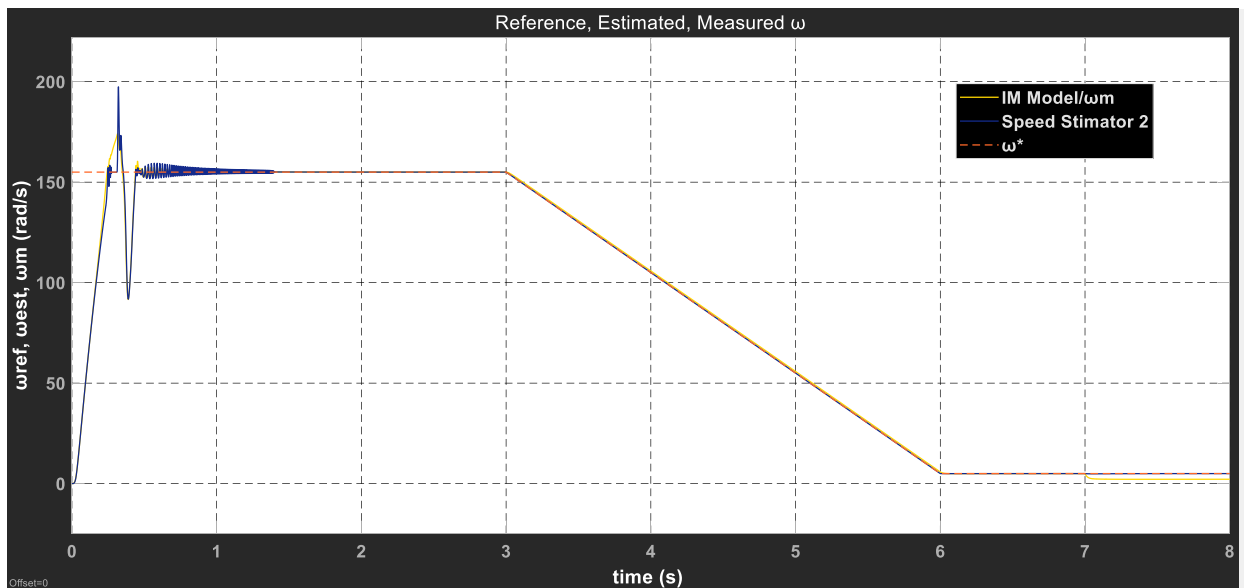


Figure 3-22 Machine, reference and Estimated Speeds for case 3.

For this case in figure 3.20 its possible to see that estimated speed have high negative and positive peaks with an overshoot of around 27% then some oscillations till steady state is achieved at  $t=1.2$  seconds. This reaction is due to the observer of the speed estimator requires the flux of the machine, at  $t=0$  the machine is not magnetized and is not possible to calculate it. This error reflects on the peaks and damped oscillations. After this, when the ramp and the load step are applied, the speed estimator works properly as it is shown in other cases.

3.6.4 Case 4: Speed step and load step. W/O Estimator.

Our fourth and final case we analyze the behavior of our model without the speed estimator. A nominal speed step is applied at t=3 seconds and after 2 more seconds a nominal load is applied. Following images show the results.

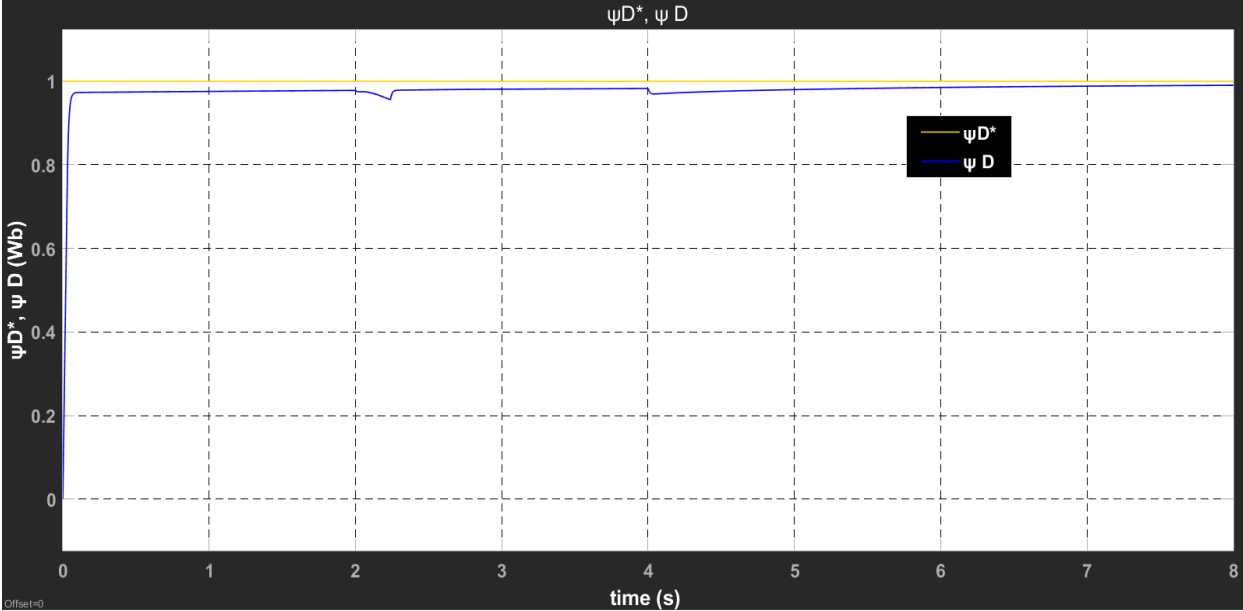


Figure 3-23 Reference and actual flux for case 4.

For this case the flux have a very steady behavior as it just decreases slightly when the speed and torque steps are applied. Note that the flux error decreases with the nominal load is running.

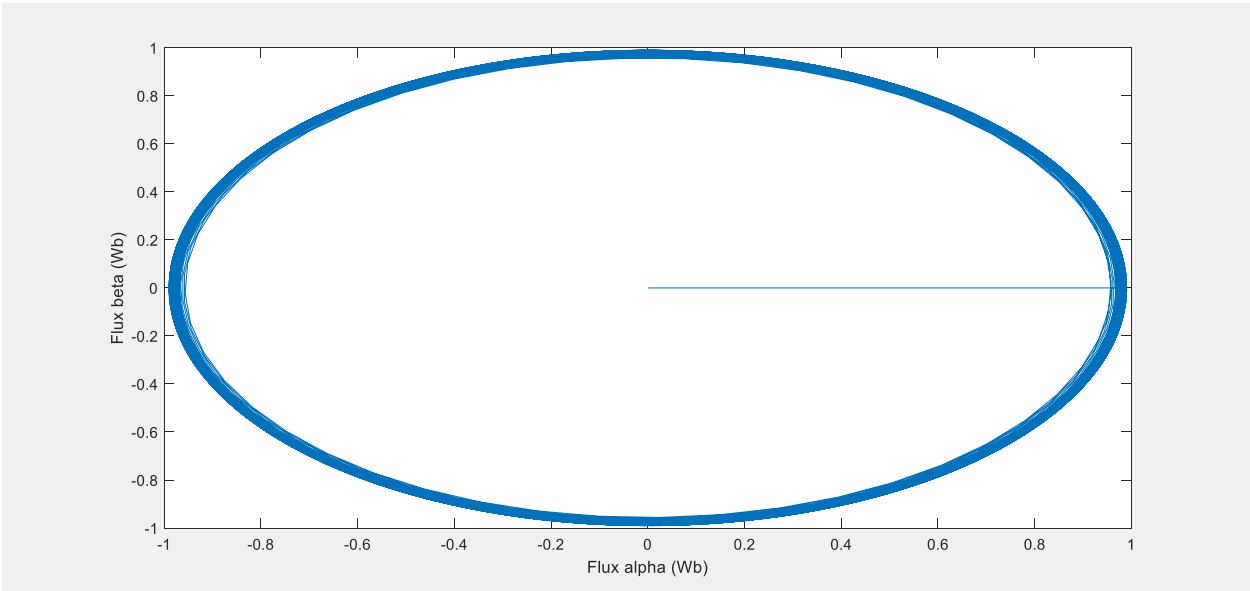


Figure 3-24 Measured Flux in polar coordinates for case 4.

The figure above shows the flux in polar coordinates. It is possible to see that the controller can keep the flux in a circular shape which means the control function is efficient.

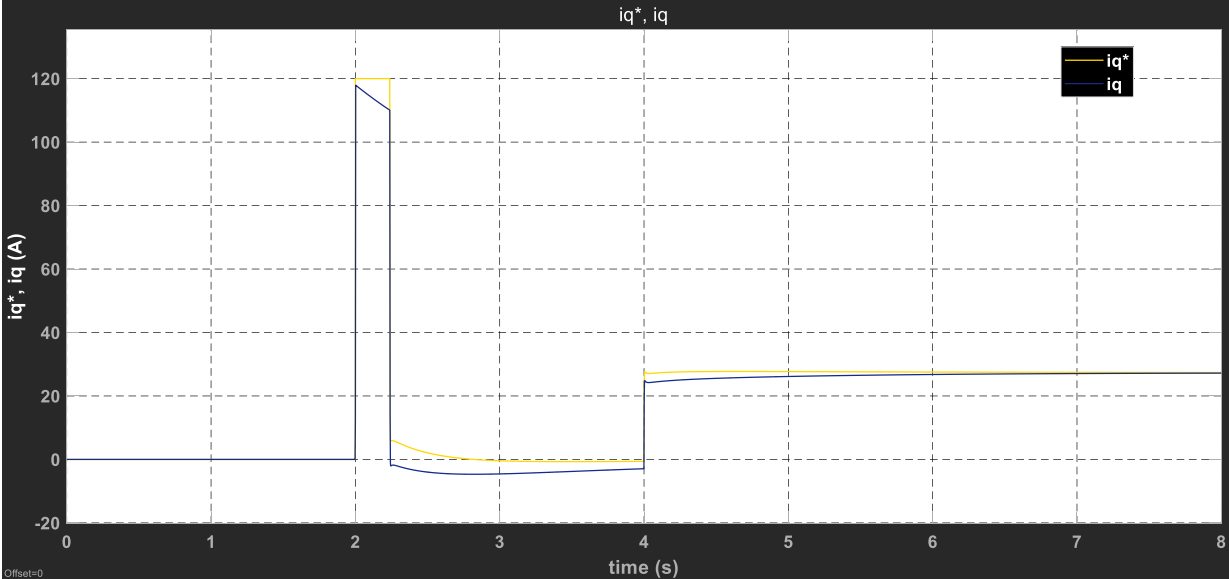


Figure 3-25 Reference and actual iq for case 4.

Quadrature current shows a similar behavior as in case 2. While the machine is in no-load regime current stays 0. When the speed step is applied it reaches a peak to break the inertial of the static rotor. When the current decreases the error between both currents is bigger but the stabilizes as the load is applied.

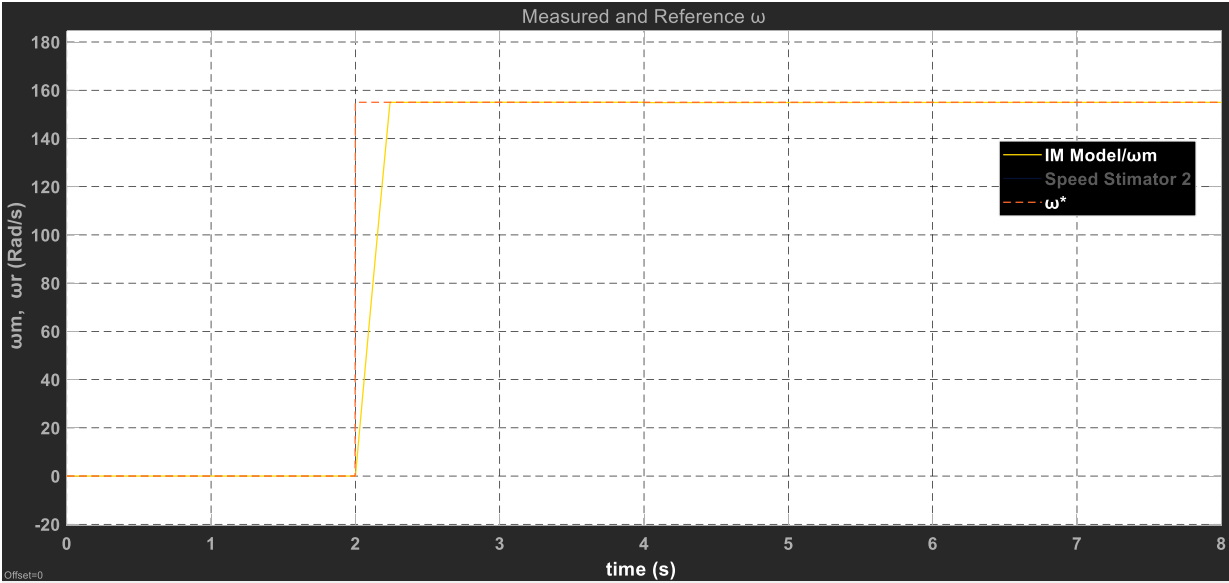


Figure 3-26 Machine and reference Speeds for case 4.

We can notice that the machine speed step reaction is slower from the reference as it is natural for this kind of systems. Also, we can see that the error is very small between reference and actual speed.

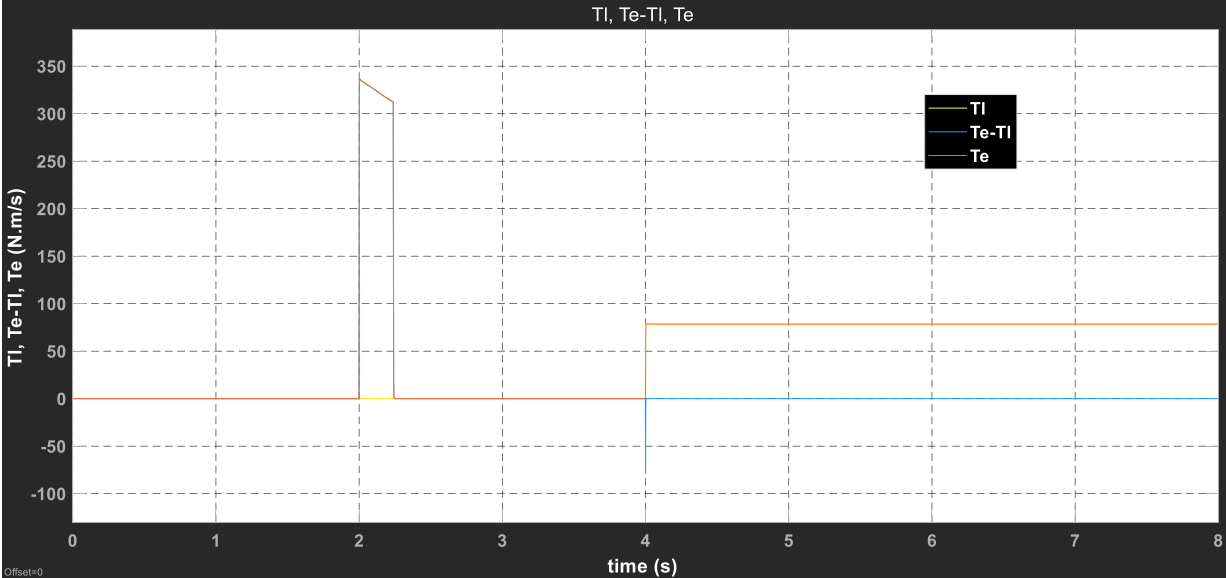


Figure 3-27 Load torque, Machine torque and Electromagnetic torque for case 4.

Torque reaction is similar to previous cases and to the quadrature current reaction. An impulse is required to move the rotor mass and is kept till the machine starts rotating to the required speed. Then, the load is applied, and the machine moves the load in steady state.

## Conclusions.

After making a study about different control methods for induction machines, we can understand the complexity of the scheme compared to a DC machine scheme even after knowing that the methodology of the control systems is to make IM behave as a DC machine. We also described that the machine can be modelled in the steady state for scalar control and the dynamic state for vector control.

For the control methods, we explored the classic control schemes of field-oriented control and direct torque control. One of the fundamental differences of these methods is the need of knowing the machine parameters. For the field-oriented control, we can see that most of machine parameters are required to obtain a good controller response as we need to estimate stator and rotor fluxes because those are the variables we should control. Another fundamental difference is the need of doing a coordinate transformation. Without these two notes, we can obtain a much simpler control scheme for DTC but for the determination of the correct vector for keeping the torque in the references, a more complex algorithm is required.

For the simulations, we determined that our controller works properly for speed ramps and load steps as we can see from images of case 1 and 2. The speed estimator provokes some undesired peaks and oscillations. This kind of errors are usually caused by machine parameters mismatch, inverter non-linearity or need of low pass filters. The first two doesn't apply for our case because we are just based on a simulation and we are not using an inverter. This could be improved by adding some limit for the flux so we can avoid those speed peaks. Many algorithms for improving the response of the estimator have been developed and other speed estimations as well. Employing closed-loop flux integration, like the reduced order observer (ROO) and the full-order Luenberger adaptive observer or Kalman filters would probably deliver better results. This could be studied in further works.

Other further works could be implementing this control in a platform such as dSpace to verify its performance on the real motor. It is also possible to implement DTC on the same machine to compare results, so the speed estimation is not necessary.

## Bibliography

- [1.] Jaulin, L. (2015). *Feedback Linearization*. Retrieved from Science Direct:  
<https://www.sciencedirect.com/topics/engineering/feedback-linearization>
- [2.] Juha Pyrhönen, V. H. (2016). *Electrical Machine Drives Control*. Wiley.
- [3.] Kovacs, P. (1984). *Transient Phenomena in Electrical Machines* . Budapest: Akademiai Kiado .
- [4.] Kundur, P. (1994). *Power System Stability and Control*. McGraw-Hill Education.
- [5.] Leonhard, W. (2001). *Control of Electrical Drives 3rd Edition*. Springer.
- [6.] Maurizio Cirrincione, M. P. (2012). *Power Converters and AC Electrical Drives with Linear Neural Networks*. CRC Press.
- [7.] Mohan, N. (2014). *Advanced Electric Drives*. John Wiley & Sons, Inc.
- [8.] Paul Krause, O. W. (2013). *Analysis of Electric Machinery and Drive Systems 3rd Edition*. John Wiley & Sons.
- [9.] Popescu, M. (2000). *Induction motor modelling for vector control purposes*. Espoo, Helsinki University of Technology.
- [10.] Vas, P. (1998). *Sensorless Vector and Direct Torque Control* . Oxford University Press.